ANALYSIS AND INTERPRETATION OF CW ARCAS ROCKET PROPAGATION EXPERIMENTS PERFORMED DURING THE NOVEMBER 2, 1969 POLAR CAP ABSORPTION EVENT

B. W. Lee, et al

Ohio State University Research Foundation

Prepared for:

Ballistic Research Laboratories
Defense Nuclear Agency

January 1974

UNCLASSIFIED

Security Classification

AD 774300

DOCUMENT CONTROL DATA - R & D

(Security classification of title, body of abstract and indexing annotation must be entered when the overall report is classified)

1. ORIGINATING ACTIVITY (Corporate author)

The Ohio State University Research Foundation
1314 Kinnear Road
Columbus, Ohio 43212

2a. REPORT SECURITY CLASSIFICATION

Unclassified

2b. GROUP

3. REPORT TITLE

ANALYSIS AND INTERPRETATION OF CW ARCAS ROCKET PROPAGATION EXPERIMENTS PERFORMED DURING THE NOVEMBER 2, 1969 POLAR CAP ABSORPTION EVENT

4. DESCRIPTIVE NOTES (Type of report and inclusive dates)

Final Report

5. AUTHOR(S) (First name, middle initial, last name)

B. W. Lee and T. A. Seliga

6. REPORT DATE	7a. TOTAL NO. OF PAGES	7b. NO. OF REFS
JANUARY 1974	62/67	42

8a. CONTRACT OR GRANT NO. DAAD5-71-C-0421	9a. ORIGINATOR'S REPORT NUMBER(S)
b. PROJECT NO. DNA MIGHTY SKY Subtask 603	Technical Report 3261-1
c. Work Unit 02	9b. OTHER REPORT NO(S) (Any other numbers that may be assigned this report)
d.	BRL Contract Report No. 132

10. DISTRIBUTION STATEMENT

Approved for public release; distribution unlimited.

11. SUPPLEMENTARY NOTES	12. SPONSORING MILITARY ACTIVITY
This research was sponsored by the Defense Nuclear Agency under MIGHTY SKY Subtask 603, Work Unit C2, Work Unit Title "Data Reduction/Analysis for Polar Cap Absorption Event Early Time Rocket Borne Instrumentation Measurement."	Director US Army Ballistic Research Laboratories Aberdeen Proving Ground, MD 21005

13. ABSTRACT

Low D region electron density profiles are deduced from the H-2, H-3, H-4, and H-6 Arcas continuous wave propagation experiments conducted at Ft. Churchill, Manitoba, Canada during the November 2, 1969 Polar Cap Absorption Event (PCA). The profiles compare favorably with others obtained during the PCA and should contribute to the total collection of data of relevant ionospheric parameters associated with the event. The results indicate a major influence of solar radiation on the ambient electron density, evident by a strong dependence of the electron density profiles on solar zenith angle.

The electron density profiles are interpreted according to simple chemical models of three-body attachment processes at night, ion-ion neutralization, and possible dissociative recombination mechanisms involving water cluster and non-water cluster ions. The nighttime effective electron loss coefficient, calculated from rocket H-2, for $60 \lesssim Z \lesssim 70$ km was found to agree favorably with the results of Swider *et al.* (1971) who showed that $\alpha_{eff} \approx L(A)/Q(Z < 75\ km)$ where $L(A)$ is the electron loss rate due to three-body attachment of electrons to O_2 and Q is the ionization production rate. The daytime results indicated that, if electron dissociative recombination is negligible in the height range below 60 km, then the values of ion-ion neutralization coefficient (α_i) were within the range thought to be consistent with water cluster reactions. Alternatively, the inclusion of electron dissociative recombination as an important process in the positive ion chemistry resulted in the determination of possible combinations of α_i and α_d (dissociative recombination coefficient) required to balance the positive ion continuity equation.

DD FORM 1 NOV 68 1473 REPLACES DD FORM 14.8, 1 JAN 64, WHICH IS OBSOLETE FOR ARMY USE.

UNCLASSIFIED

Security Classification

14. KEY WORDS	LINK A		LINK B		LINK C	
	ROLE	WT	ROLE	WT	ROLE	WT
Polar Cap Absorption						
Ionosphere						
Continuous Wave Propagation						
Electron Density						
Attachment Processes						
Neutralization						
Dissociative Recombination						

ANALYSIS AND INTERPRETATION OF CW ARCAS ROCKET PROPAGATION EXPERIMENTS PERFORMED DURING THE NOVEMBER 2, 1969 POLAR CAP ABSORPTION EVENT

B. W. Lee

T. A. Seliga

CONTRACT REPORT NO. 132

JANUARY 1974

TECHNICAL REPORT 3261-1

Contract No. DAADO 5-71-C-0421

The material used in this report is also used as a thesis submitted to the Department of Electrical Engineering, The Ohio State University in partial fulfillment for the degree of Master of Science.

The Ohio State University
The Department of Electrical Engineering
and
The Atmospheric Sciences Program
Columbus, Ohio

This research was sponsored by the Defense Nuclear Agency under MIGHTY SKY Subtask 603, Work Unit 02, Work Unit Title "Data Reduction/Analysis for Polar Cap Absorption Event Early Time Rocket Borne Instrumentation Measurement."

Ballistic Research Laboratories

Aberdeen Proving Ground, Maryland 21005

TABLE OF CONTENTS

LIST OF TABLES

LIST OF FIGURES

CHAPTER I

INTRODUCTION

1.1 Polar Cap Absorption Event

The purpose of this work is to determine and analyze the electron density variations in the ionosphere during the November 2, 1969 Polar Cap Absorption Event.

Polar cap absorption (PCA) refers to an abnormal absorption of high frequency radiowaves propagating through a disturbed D region of the ionosphere at polar geomagne titudes. This particular ionospheric disturbance has been attributed to solar flare emissions of predominately subrelativistic protons in the energy range of 5-30 Mev which journey from the sun through interplanetary space and approach the earth. In their approach toward the earth, the earth's magnetic field deflects and focuses these solar particles toward the polar regions where they penetrate the earth's upper atmosphere and ionize the atmospheric constituents in the altitude range of about 45-75 km. The resultant increase in the ambient electron density in the D region results in the detrimental absorption of radiowaves which greatly limits the use of high frequency radio and radar

communications for several days after the associated solar disturbance (flare) has passed.

Research on PCA phenomena has been stimulated not only by the need to understand the deleterious effects on communications, but also by opportunities presented by the PCA to study the unfamiliar and complex chemistry of the D region under highly disturbed conditions. One of the opportunities available is the chance to obtain reliable D region electron density profiles.

During the PCA, because of the increase in the ionization of the D region, the absorption of high frequency radiowaves propagating through the lower ionosphere is quite sensitive to the D region electron concentration. This sensitivity makes possible the use of radio absorption measurements as a reliable analytical tool for determining the D region electron density. This ionospheric parameter along with other available information such as derived electron-ion production rates during a PCA event, aids in the formulation and testing of chemical models. which in turn lead toward a better understanding of ionospheric mechanisms; these include ion-electron formation and neutralization, ion-electron recombination, ion-ion neutralization, and electron attachment and detachment in the lower ionosphere. An excellent review of the PCA phenomenon was given by Bailey (1964) who discussed in detail most of the important related ionospheric observations and our understanding of them.

1.2 Operation PCA-69

Toward resolving some of the questions concerning the D region processes, the Defense Nuclear Agency (DNA) initiated an aeronomical research program designated Operation PCA-69. The program coordinated efforts for the measurement of various ionospheric changes during a PCA event by rocket, satellite, aircraft, and ground based instruments. The objectives of these measurements were to acquire specific data on the ionospheric changes resulting from the sudden influx of energetic protons into the atmosphere and the subsequent effects of these changes on high frequency communications.

The rocket segment of PCA-69 consisted of a series of scientifically instrumented rockets launched from the Churchill Research Range at Ft. Churchill in Manitoba, Canada during the November 2, 1969 PCA event. Prior to the solar event, eleven rockets were fired to provide background information on the ionospheric conditions and to provide certification of the equipment. Thirty-six rockets were launched to provide measurements during the progress of the PCA. Rocket borne instruments measured the flux of energetic protons, electrons, and alpha particles into the atmosphere; the radiation intensities of X-rays and Lyman alpha; and atmospheric effects of ionization, light emissions, and heating (Ulwick; 1971).

1.3 PCA-69 Arcas Rocket Experiments

As part of the rocket segment of PCA-69, the Ionospheric Research Laboratory of the Pennsylvania State University launched nine Arcas rockets designated H-1 to H-9 on November 3 and 4, 1969 to obtain data on electron and ion densities for the study of the physical chemistry of the D region during the PCA sunrise-sunset period. Preliminary assessment of the data from these flights was given by Hale and Seliga (1970).

All nine rockets contained a parachute borne blunt probe experiment to measure charged particle conductivities which can be used with available data on charged particle mobilities and meteorological conditions to determine charged particle densities. Hale (1967) and Hale et al (1968) described in detail the blunt probe theory and measurements. From the Arcas blunt probe measurements, Hale et al (1971) deduced the charge particle densities during the November 2, 1969 PCA event. These data are used later in this work to aid in the interpretations of D region PCA events.

Except for H-9, the Arcas rocket also contained a CW propagation experiment which was to be operational during ascent and jettisoned at apogee, after which the parachute borne blunt probe experiment functioned on descent by parachute. The propagation experiment was designed to determine the electron density in the low D region of the ionosphere by the measurement of the absorption of a 3.65 MHz CW

signal transmitted from the ground to the rocket. The Ionosphere Research Laboratory conducted the experiments and processed the telemetry data to obtain the signal strength received by the rockets during their flight (Melrose and Hale; 1970). Of the eight flights which contained propagation experiments, four yielded reliable data from which electron densities could be deduced. Pertinent data concerning these four flights are given in Table 1-1.

1.4 Objectives

In this work the absorption data obtained from the propagation experiments from the rocket flights of H-2, H-3, H-4, and H-6 are used to determine electron density profiles using numerical full wave techniques based on the generalized magnetoionic equations. Comparison of the deduced electron density profiles is made with those of Dean (1971). The resultant profiles are interpreted in light of possible processes occurring in the low D region during the PCA event, using the complementary positive ion measurements of Hale et al (1971) and preliminary calculations of production rates of Swider and Gardner (1972).

TABLE 1-1

PERTINENT DATA ON THE FOUR ARCAS FLIGHTS FROM WHICH ELECTRON DENSITIES ARE DEDUCED

ARCAS FLIGHT	LOCAL TIME OF LIFTOFF		SOLAR ZENITH ANGLE	AZIMUTH ANGLE	APOGEE ALTITUDE	APOGEE RANGE
H-2	0100	3 Nov 1969	134.8°	128.0°	67.2 km	24.1 km
H-3	0628	3 Nov 1969	99.1°	121.5°	64.1 km	21.3 km
H-4	0805	3 Nov 1969	87.7°	136.2°	64.7 km	20.5 km
H-6	1343	4 Nov 1969	77.2°	333.5°	68.7 km	7.9 km

CHAPTER II

ARCAS CW PROPAGATION DATA

2.1 CW Propagation Experiments

The CW propagation experiment is specifically designed for use with small rockets to determine electron densities in the D region. The basic measurement in such an experiment is the magnetic and/or electric field amplitude of a radiowave transmitted from the ground to a narrow band receiver on the rocket traversing the ionosphere. A rocket borne telemetry system transmits the information of the received signal amplitude to a ground station where data is processed and analyzed to determine electron densities when the collision frequency profile is either known or assumed (Bowhill and Mechtly; 1961).

Hall (1964) and Seliga (1968) performed CW propagation experiments to find D region electron densities by measurement of a specific amplitude parameter and by use of a full wave solution to calculate the parameter based on several electron density models. The electron density profile which gave a field parameter comparable to the measured value was taken as the profile representing the state of the ionosphere at the time of the flight. The work by Hall and Seliga

demonstrated the usefulness of the relatively simple CW propagation technique in determining electron densities in the D region.

2.2 Details of the Arcas CW Propagation Experiment and the Reduction of Data for Analysis

The Arcas CW propagation experiment consisted of a 3.65 MHz radiowave radiated from the ground by a horizontal half-wave dipole to a rocket as it passed through the ionosphere. The transmitters were located at the launch site. In the rocket a single ferrite rod antenna, oriented perpendicular to the rocket axis, detected the magnetic field strength of the wave in a plane nearly parallel to the earth's surface and served as a signal source to the receiver. Since the rocket spun at a rate of about 10 to 20 Hz, the receiver output was modulated not only by the ionospheric effects of absorption and Faraday rotation, but also by the spinning action of the rocket.

An example of the signal received by a rocket in flight is illustrated in Figure 2-1, which is a segment of the processed telemetry signals from the H-6 flight. The frequency at which the nulls appear is about twice the rocket spin frequency; the actual difference between the spin rate and occurrence of the nulls would be due to Faraday rotation, a rotation of the plane of polarization of the radiowave as it propagates upward through the ionosphere. It should be noted that, although planned, Faraday rotation measurements were not possible because of the failure of the ground based telemetry receiver to produce adequate

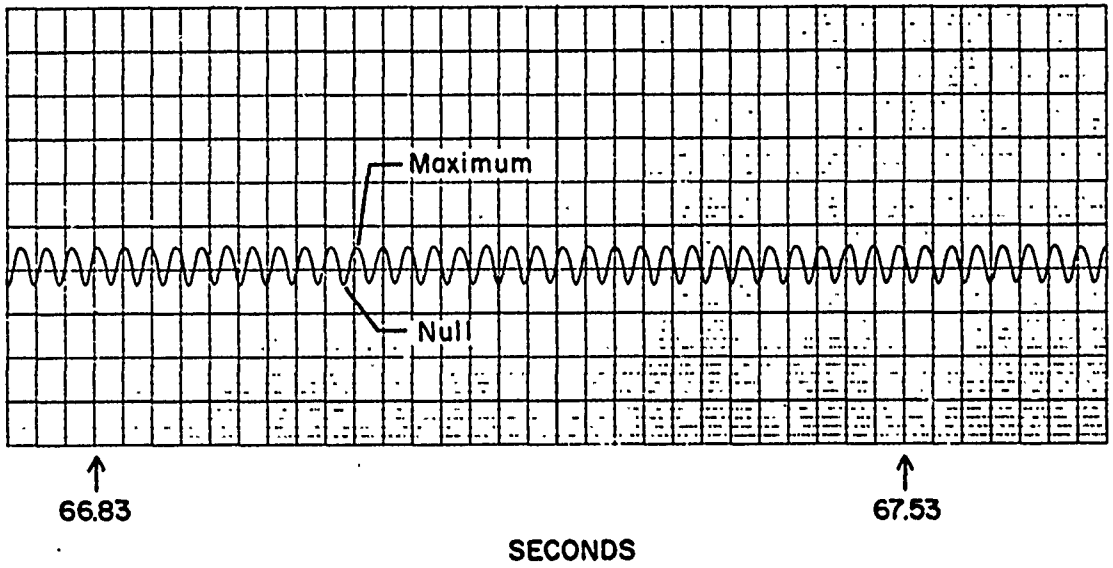

Figure 2-1. Sample of signal received by the H-6 Arcas rocket.

automatic gain control signals whose variation could be used to indicate rocket spin rate as a reference. The maximum signal occurs at the points where the orientation of the ferrite rod antenna couples most effectively to the magnetic field of the wave. Therefore, for a rocket having its axis aligned nearly along the straight line path from the transmitter, the maximum signal received at the rocket would coincide with the maximum magnetic field intensity in the plane normal to the direction of propagation; this is the case for the Arcas experiments.

This maximum magnetic field strength was selected as the measured parameter to be used with the full wave solution to deduce the electron density profiles. This choice was made because the maximum was a consistent point that could easily be determined from the waveform of the received signal and because the maximum was probably the most accurate value detected by the receiver. In practice it was found that the relative absorption rates calculated from the full wave solution for conditions of each of the rocket trajectories, using the same electron density profile and accounting for expected variances due to the differences in the angle of incidence, were not significantly different from one another. In addition, the calculated rates were practically the same as rates obtained from the maximum horizontal magnetic field intensity for an incident wave magnetically polarized normal to the plane of incidence. This latter observation

considerably simplified the otherwise important geometrical factors involved in calculating the desired field parameter. It should also be noted that the non-sensitivity of the calculations to propagation direction is expected at Ft. Churchill because of the propagation conditions associated with the near vertical geomagnetic field.

Plot I of Figures 2-2a to 2-2d shows the maximum relative magnetic field strength as received by each of the four rockets passing through the lower ionosphere. It should be noted that this signal is composed of three components: the first is the component due to the ionospheric absorption of the radiowave; the second is that due to the spreading loss (1/R); and the third, due to the transmitting antenna pattern. For the analysis, the ionospheric absorption component is required and must be extracted from Plot I for each flight.

Using the radar tracking data for flights H-2, H-3, H-4, and H-6, the relative spreading loss was calculated for each flight and added to Plot I of the corresponding figure. Plot II of Figures 2-2a to 2-2d shows the maximum magnetic field strength after spreading loss was accounted for. Any compensation of loss due to the transmitting antenna pattern was neglected since each rocket flew at approximately the same azimuth and elevation angles throughout its flight in the altitude region of interest; the antenna pattern would then yield an almost constant signal loss with altitude. Since only relative absorption was required for electron density determination, ignoring this

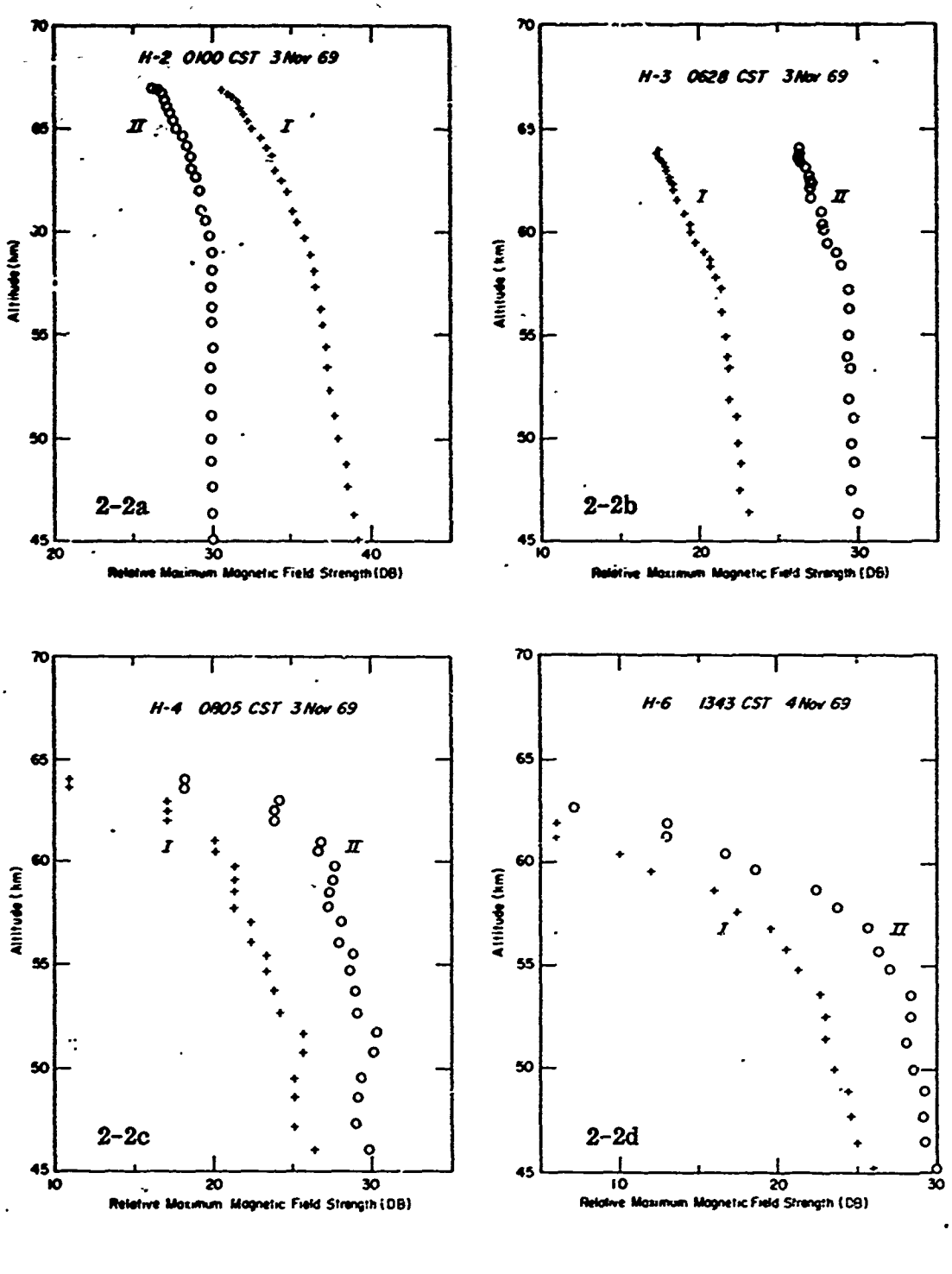

Figures 2-2a to 2-2d. Relative maximum magnetic field strength measured from the H-2, H-3, H-4, and H-6 telemetry data. Plot I indicates the maximum field strength as received by each rocket during its flight; Plot II, the field strength after spreading loss is added to that of Plot I.

constant loss would not influence the final results. Therefore, this and the above noted observations on the results of calculated magnetic field intensities for different propagation conditions allow us to consider Plot II of Figures 2-2a to 2-2d as the relative ionospheric absorption of the maximum horizontal component of the magnetic field intensity of a linearly polarized CW signal incident on the ionosphere.

Table 2-1 gives the absorption rates for each rocket flight in decibels per kilometer derived by curve fitting the points given in Plot II. These measured rates which are independent of the absolute field strength of the wave represent the reduced data, analyzed by the full wave technique.

TABLE 2-1

ABSORPTION RATES (db/km) DEDUCED FROM THE ARCAS DATA

ALTITUDE (km)	ROCKET FLIGHT H-2	H-3	H-4	H-6
50			0.09	0.16
51			0.10	0.18
52			0.12	0.23
53		0.009	0.14	0.33
54		0.02	0.18	0.50
55		0.05	0.20	0.76
56		0.10	0.23	1.08
57		0.14	0.30	1.45
58		0.27	0.40	2.00
59	0.10	0.35	0.46	2.55
60	0.16	0.42	0.65	3.12
61	0.22	0.48	0.90	3.75
62	0.32	0.54	1.32	4.50
63	0.43	0.65	1.80	5.00
64	0.53	0.76		
65	0.60			
66	0.71			
67	0.81			

Note: these rates are the absolute value of the actual rates which are negative numbers.

CHAPTER III

ANALYSIS OF DATA

3.1 Analytical Full Wave Technique

The analysis of the data obtained from the propagation experiments is based on the numerical solution of the governing differential equations of a plane wave obliquely incident from free space on a horizontally stratified ionosphere. Budden (1955) presented these basic magneto-ionic equations and discussed the procedure by which the reflection coefficients can be obtained from their numerical integration. Pitteway (1965) and Seliga (1966) extended the numerical solution for use in analyzing rocket data. Seliga (1966) included the generalized formulation of the governing equations which accounts for the dependence of the electron collision frequency on electron energy as discovered by Phelps and Pack (1959) and analytically treated by Sen and Wyller (1960). A computer program of the full wave technique as outlined by Seliga (1966) was written for analysis of the data obtained from the Arcas rocket flights.

The program may be altered to calculate any field parameter desired, but for the analysis of the Arcas data the maximum magnetic

field intensity in the horizontal plane for a wave propagating in the region of the ionosphere where measurements were made was used. This region was assumed to be bounded above and below by a homogeneous medium. Below the region of interest, the medium is characterized by a refractive index having a real part within 3% of unity and an imaginary part not greater than 0.0003. For the purpose of this analysis, such a region was considered as free space: these limits are consistent with those considered by Budden (1955).

Above the region of interest, the electron density and collision frequency were assumed to be constant with altitude. This assumption implies that any reflections, occurring above the region of interest and which may contribute to the total wave field in the region of interest, are negligible. For the Arcas experiments this assumption is valid, since no standing waves were observed in the wave field data (Figure 2-2a to 2-2d), indicating that the amplitude of any reflected wave was negligible compared to the upgoing wave. Therefore, the upper boundary condition of constant electron density and collision frequency does not affect the wave solutions in the region of interest, but does provide an important artificial physical condition for numerical calculation of the actual wave fields.

These physical conditions imposed on the region establish the mathematical boundary conditions by which a numerical solution of the differential equations can uniquely be determined for an incident CW

signal of known polarization. For each of the flights, the incident wave was linearly polarized with transmission emanating from a horizontal electric dipole aligned in the East-West direction. Other parameters required for the full wave solution include a monoenergetic electron collision frequency profile, the geomagnetic field, the wave frequency, the angle of incidence, and assumed electron density profiles. The fixed parameters for the Arcas experiments are outlined in Table 3-1.

Since the single frequency CW propagation experiment is incapable of determining an independent measure of the electron collision frequency, an assumed model, shown in Figure 3-1, was required. This collision frequency was the same model used by Seliga (1968) in analysis of a low frequency propagation experiment at Ft. Churchill in the summer of 1963. This model is representative of several experimental measurements of collision frequency. Its value is given by

$$\nu_m = 3.5 \times 10^6 \exp\left(-\frac{z-70}{6.6}\right) \ \text{sec}^{-1}$$

where z is the altitude in kilometers.

3.2 Procedure for Determination of Electron Density

In order to determine the electron density profile an iterative procedure was used based upon absorption rates calculated from the full wave solution using appropriate electron density profiles. The procedure is outlined below:

1. A series of contour plots of absorption rate versus altitude for a given electron density were obtained from full wave

TABLE 3-1

FIXED PARAMETERS USED IN THE FULL WAVE ANALYSIS OF THE ARCAS CW PROPAGATION EXPERIMENTS

ROCKET	APPROX. ANGLE OF INCIDENCE	HORIZONTAL AZIMUTH ANGLE DEFINING PLANE OF INCIDENCE	COMMON PARAMETERS
H-2	17.5°	128.0°	Wave Frequency: 3.65 MHz
H-3	15.7°	121.5°	Collision Frequency: $\nu_m = 3.5 \times 10^6 \exp\left[-\frac{z(km)-70}{6.6}\right] sec^{-1}$
H-4	14.0°	136.2°	Approximate Geomagnetic Field:
H-6	0.0°	333.5°	$\bar{B} \approx (0.64\,\bar{a}_{north} + 0.21\,\bar{a}_{east} + 6.1\,\bar{a}_{down}) \times 10^{-5}$ weber/m^2

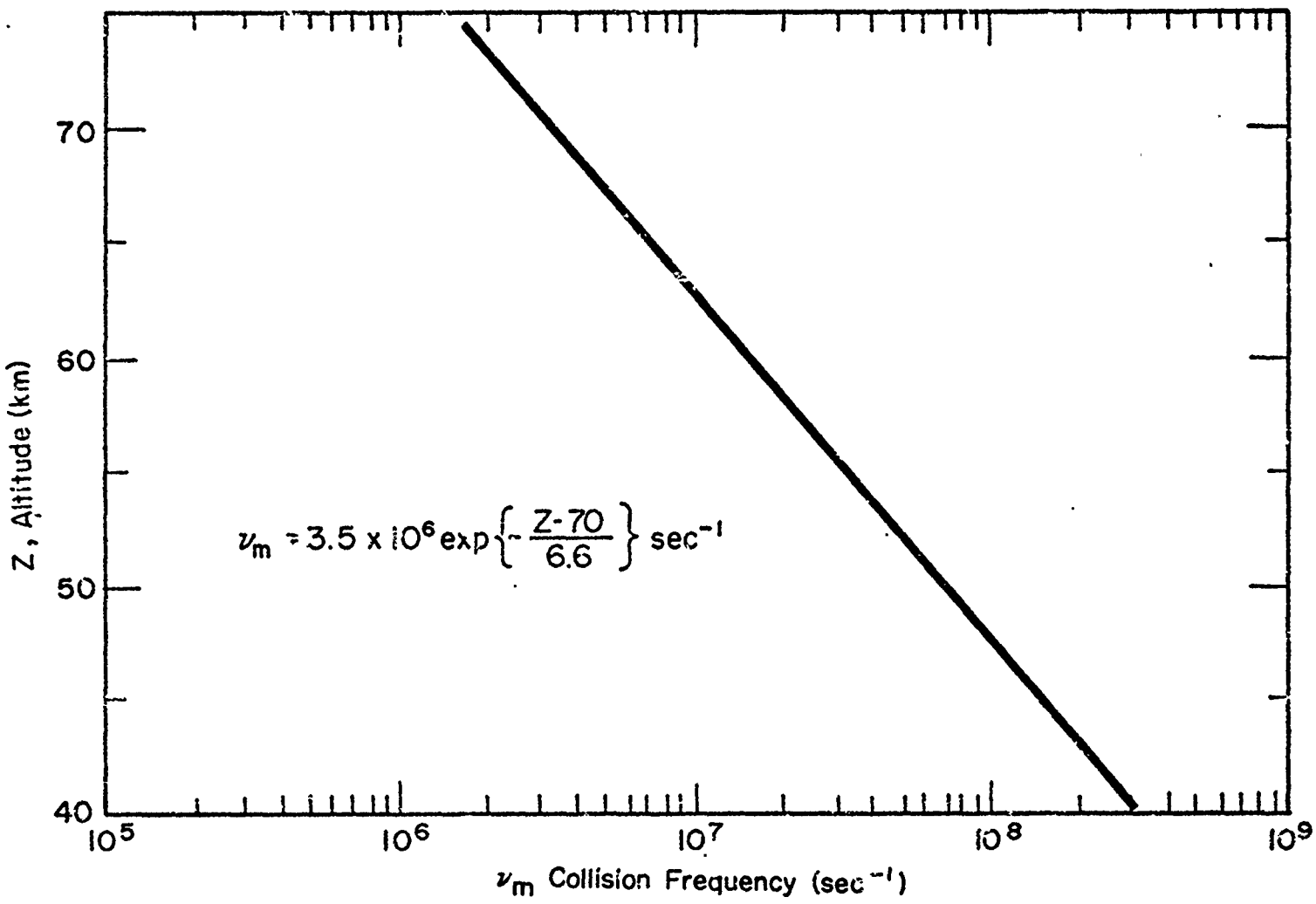

Figure 3 - 1. Electron collision frequency model used in full wave analysis.

solution computations (Fig. 3-2). These calculated data correspond to the absorption of a linearly polarized wave at 3.65 MHz, incident normally on an ionosphere having a constant electron density in the height region of interest and propagating under longitudinal conditions. These conditions approximate those for each of the rocket flights at Ft. Churchill.

2. The measured absorption rates were superimposed over the contour plots of Figure 3-2. The intersection of these curves with the contours gave the initial estimate of electron density versus altitude for the respective rocket flights.

3. The actual conditions of each flight were then imposed on the propagation conditions and full wave solutions were obtained to compare calculated absorption rates with the measured rates. Each profile was then altered assuming a linear dependence of absorption rate on electron density as a correction. The full wave solutions were repeated using the corrected electron density profile; rates were again compared, and the procedure was repeated until the rates were within three significant figures of each other. The final profiles were then presumed to be the electron density in the ionosphere at the time of their respective flights.

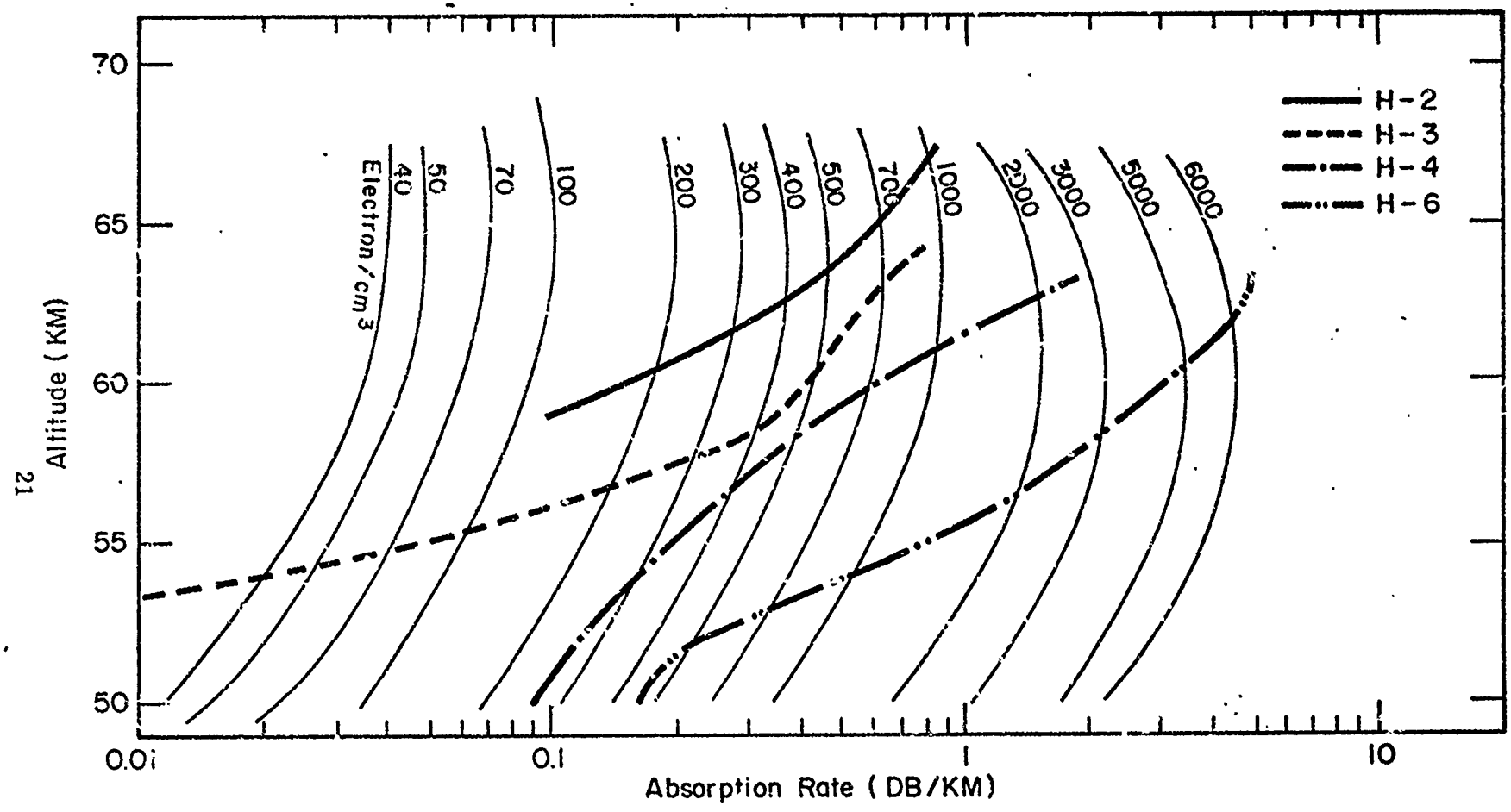

Figure 3-2. Contour plots used in determining the initial electron density profile for each flight.

3.3 Electron Density Results

The electron density profile for each flight deduced by the iterative routine described above is shown in Figure 3-3. The error is estimated to be within $\pm$ 25% of the deduced values.

The results of the rocket flights H-2, H-3, and H-4 show the night-to-sunrise transition for November 3, 1969. These profiles show an increase in electron density with decreasing solar zenith angle most likely as a result of increased photodetachment of electrons from negative ions. Comparing the results of H-2 which is a nighttime flight with that of H-3, a pre-sunrise flight, it is observed that above approximately 63 km the increase in the results of H-3 over that of H-2 is smaller than the increase below this height. This observation, assuming little or no change in the production rate, demonstrates that the mechanism causing the increase in electron density with decreasing zenith angle becomes more important with decreasing altitude.

Comparison of the results of H-4 and H-6 on November 3 and 4 respectively shows that, although the electron production rate due to the influx of energetic protons usually decreases with the progress of the PCA, the influence of solar radiation must be significant at low altitudes in order to account for the nearly factor of five increase in the electron density between around 55 and 63 km. The strong dependence of these profiles on the solar zenith angle is consistant with other observations of PCA's.

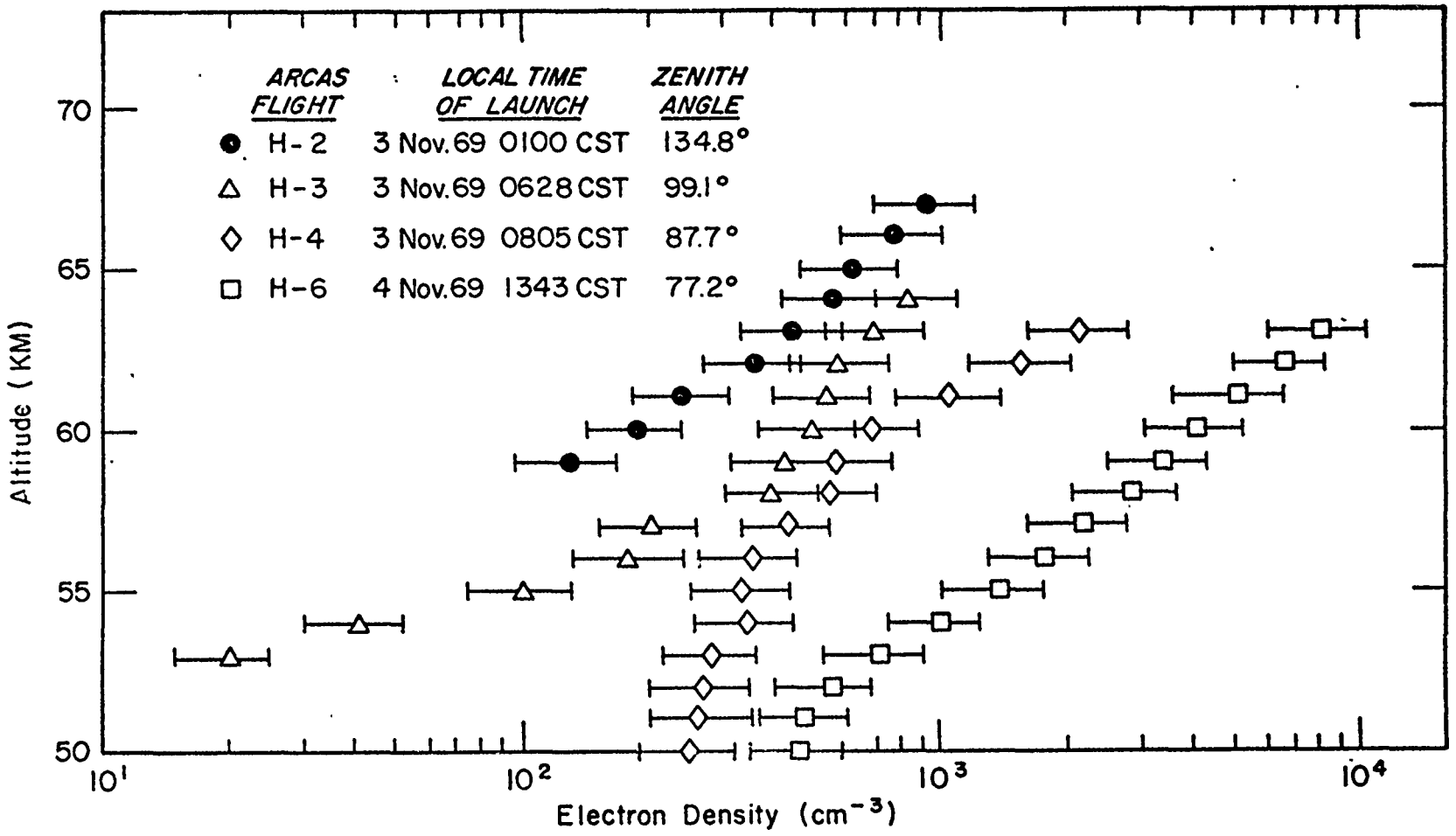

Figure 3-3. Electron density profiles deduced from the Arcas CW propagation experiments.

From riometer absorption records during the July 3-5, 1957 PCA Reid and Collins (1959) observed that this solar control of the electron detachment mechanism was not predominately dependent on visible radiation as evident by their observations that the steady state ionospheric nighttime condition was reached prior to true sunset--the time at which the sun's rays are blocked by the earth. This observation led Reid and Leinbach (1961) to suggest that the dominant negative ion in the D region during twilight was not O_2^-, since visible radiation is so efficient in detaching an electron from this ion that if it were present in large numbers, the detachment process would be quite dependent on the visible band of the solar spectrum. The work of Reid (1961) gave support to this suggestion. By assuming that O_2^- was the dominant negative ion, Reid calculated theoretical absorption curves as a function of solar zenith angle and compared them with riometer absorption measurements of a PCA during twilight. The lack of agreement between the calculated and measured results led him to conclude that the O_2^- hypothesis alone was inadequate to explain observed twilight variations in the riometer absorption. To explain the observed variation, he suggested the existence of an unknown ion X^- which would require ultraviolet radiation for detachment. As yet, the identity of X^- has not conclusively been determined, but as research continues, the behavior of this unknown ion or ions should become better known and possibly identified.

From the results of the Arcas flights H-2, H-3 and H-4, it appears that if photodetachment is responsible, the unknown negative ion producing the increase in electron density by detachment dominates below 60 km and/or the detachment process is more efficient below this height. Both of these hypotheses are supported by the electron density results.

The Arcas electron density profiles compare reasonably well with the results of Dean (1971) who performed similar rocket propagation experiments during the same period of the PCA. These comparisons are shown in Figure 3-4. The solar control which is evident by the increase in electron density with decreasing solar zenith angle is also noted in his profiles at low altitudes.

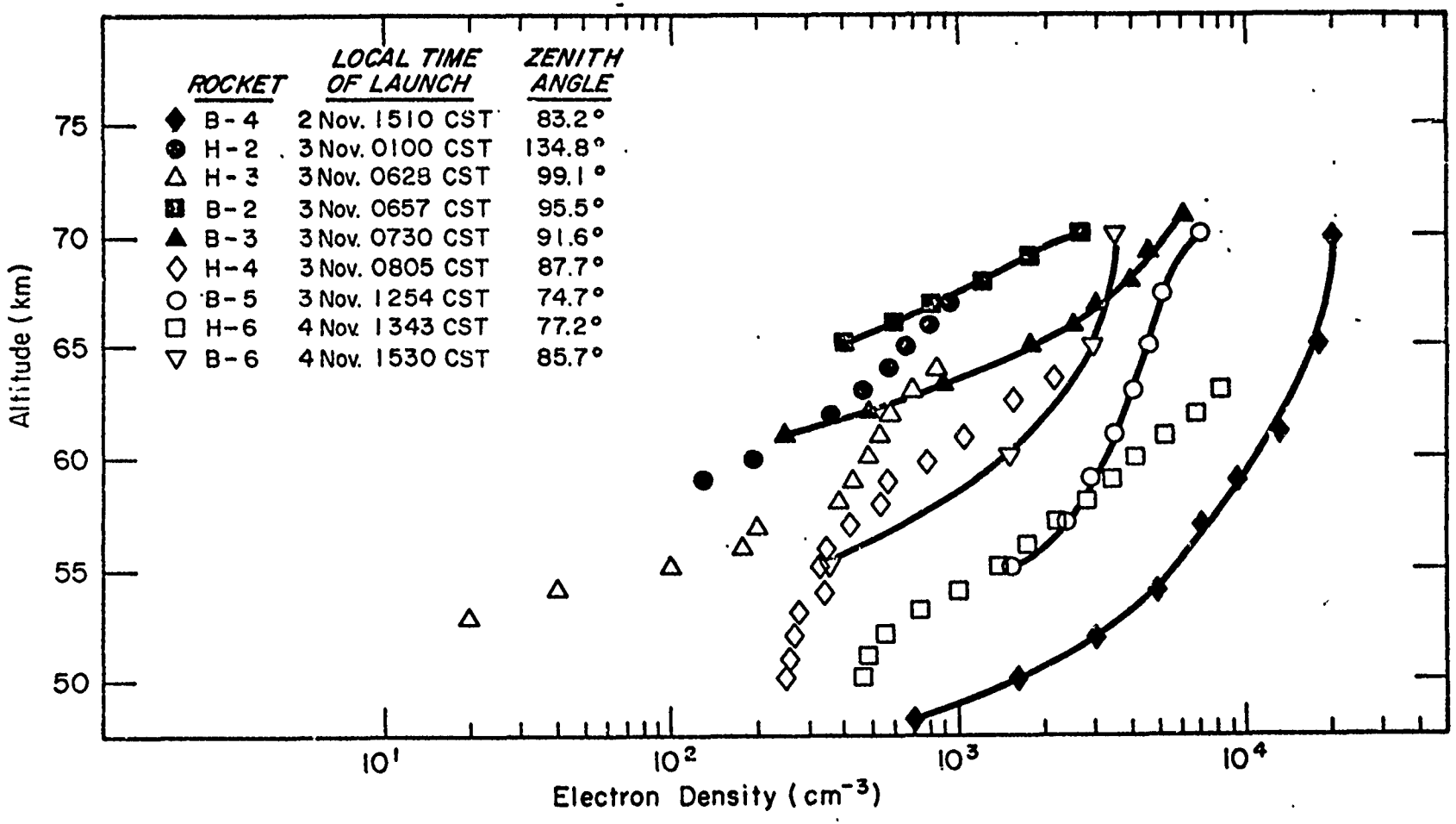

Figure 3-4. Comparison of the Arcas electron density results with Dean's (1971).

CHAPTER IV

INTERPRETATION OF THE ARCAS ELECTRON DENSITY PROFILES

4.1 Continuity Equation in the Lower Ionosphere

The D region of the ionosphere is a very difficult region to understand, being complicated by a large concentration of various species and their many possible reactions. To overcome the complexities, macroscopic reactions are considered which essentially lump the numerous reactions of the different species into equivalent reactions involving the total electron and positive and negative ion concentrations. The continuity equations of the lower ionosphere, neglecting any transport processes, are the following well-known classical differential equations (Whitten and Poppoff; 1971):

$$\frac{dN}{dt} = Q + \rho_p N_- + \rho_a N_- - AN - \alpha_d N N_+ \qquad (4.1)$$

$$\frac{dN_-}{dt} = AN - \rho_p N_- - \rho_a N_- - \alpha_i N_- N_+ \qquad (4.2)$$

$$\frac{dN_+}{dt} = Q - \alpha_d N N_+ - \alpha_i N_- N_+ \qquad (4.3)$$

where

N = total electron density (cm^{-3})

N_- = total negative ion density (cm^{-3})

N_+ = total positive ion density (cm^{-3})

Q = total electron-ion pair production rate (cm^{-3}-s^{-1})

ρ_p = photodetachment rate coefficient (s^{-1})

ρ_a = associative detachment rate coefficient (s^{-1})

A = attachment rate coefficient (s^{-1})

α_d = dissociative recombination coefficient (cm^3-s^{-1})

α_i = ion-ion neutralization (recombination) coefficient (cm^3-s^{-1})

Assuming quasi-equilibrium conditions, the time derivatives become negligible, and the effects of the ionospheric reaction chemistry can be consolidated into an effective recombination coefficient, α_{eff}, related to the electron and ion concentrations by

$$N = \left[\frac{Q}{\alpha_{eff}}\right]^{1/2} \tag{4.4}$$

with $$\alpha_{eff} = (1+\lambda)(\alpha_d + \alpha_i \lambda) \tag{4.5}$$

and $$\lambda = \frac{N_-}{N} = \frac{A}{\rho_p + \rho_a + \alpha_i N_+} \tag{4.6}$$

The parameters α_{eff} and λ are characteristic parameters of the ionosphere at a given time and condition. These parameters can be calculated from the Arcas electron density results and available data on the total electron-ion production rates and ion densities.

4.2 Calculation of the Effective Recombination Coefficient

Swider and Gardner (1972) calculated preliminary electron-ion pair production rates from proton flux measurements at four different

times during the PCA. These rates are shown in Figure 4-1 which seem to be relatively constant with height in the altitude range of interest, 45-70 km.

During the PCA the ionization due to the flux of solar protons is so much greater than any present under normal conditions that it is usually assumed to be the only ionization source responsible for the production of electrons (Bailey; 1964). Using this assumption, Figure 4-1 then represents the total electron production rates in the ionosphere at the times specified by Swider and Gardner.

In order to calculate α_{eff}, the total production rates at the time of the four Arcas flights are required. These rates were estimated by plotting the production rates, deduced by Swider and Gardner, versus time and then extrapolating between the measured points. The results of this extrapolation are shown in Figure 4-2. The validity of the procedure used in estimating the production rates during the Arcas flights depends upon the assumption that the production rate decreases monotonically during the course of the PCA. Such a decrease is reasonable in light of experimental evidence indicating that the flux of protons, with energy greater than 3 MeV, which are primarily responsible for the ionization at altitudes between 45 and 70 km, decreased continuously during the period of the Arcas flights. The proton flux measurements during this PCA from the Vela Satellite are shown in Figure 4-3 (Ulwick; 1971/ courtesy of S. Singer, Los Alamos Scientific Laboratories).

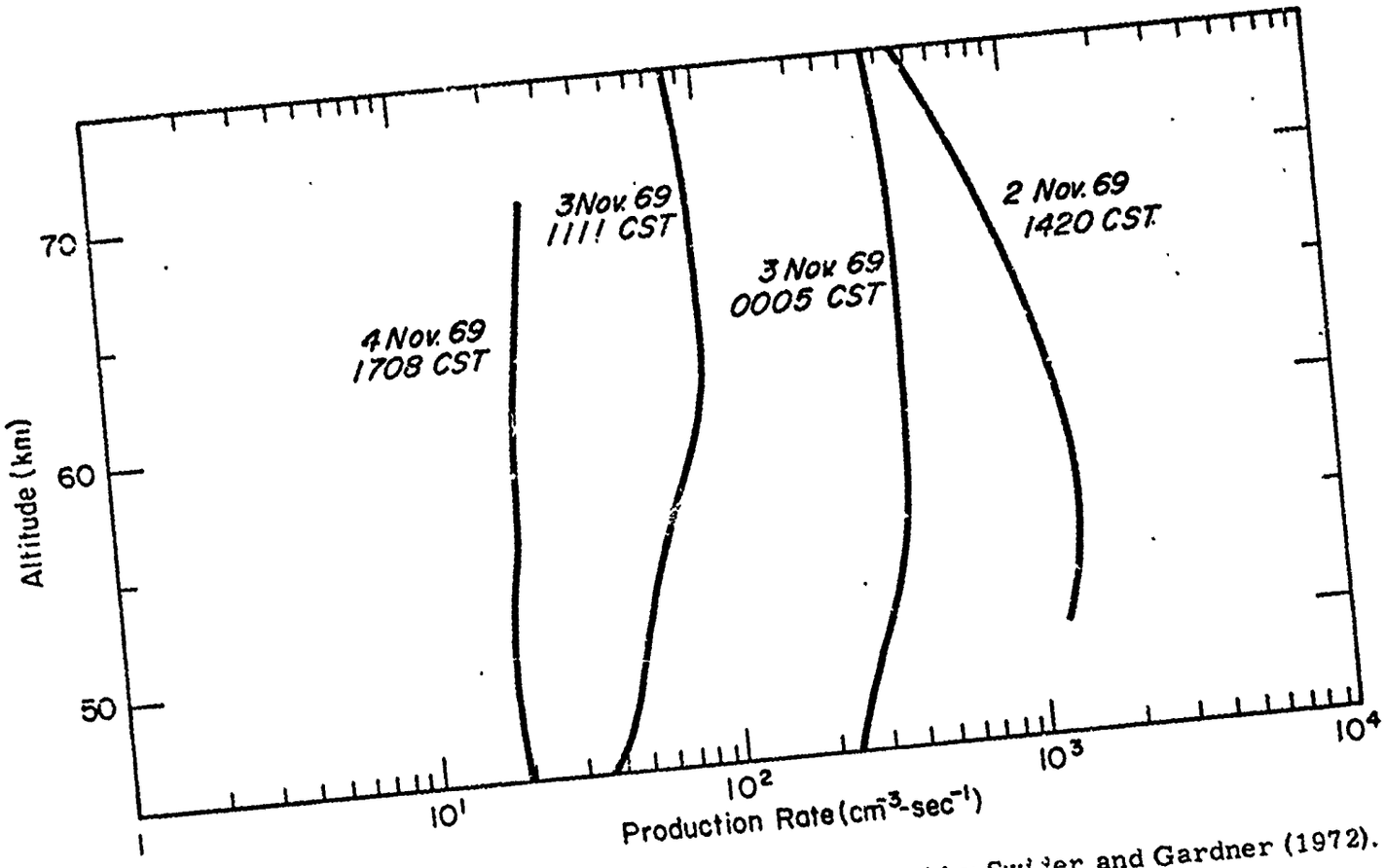

Figure 4-1. Preliminary production rates calculated by Swider and Gardner (1972).

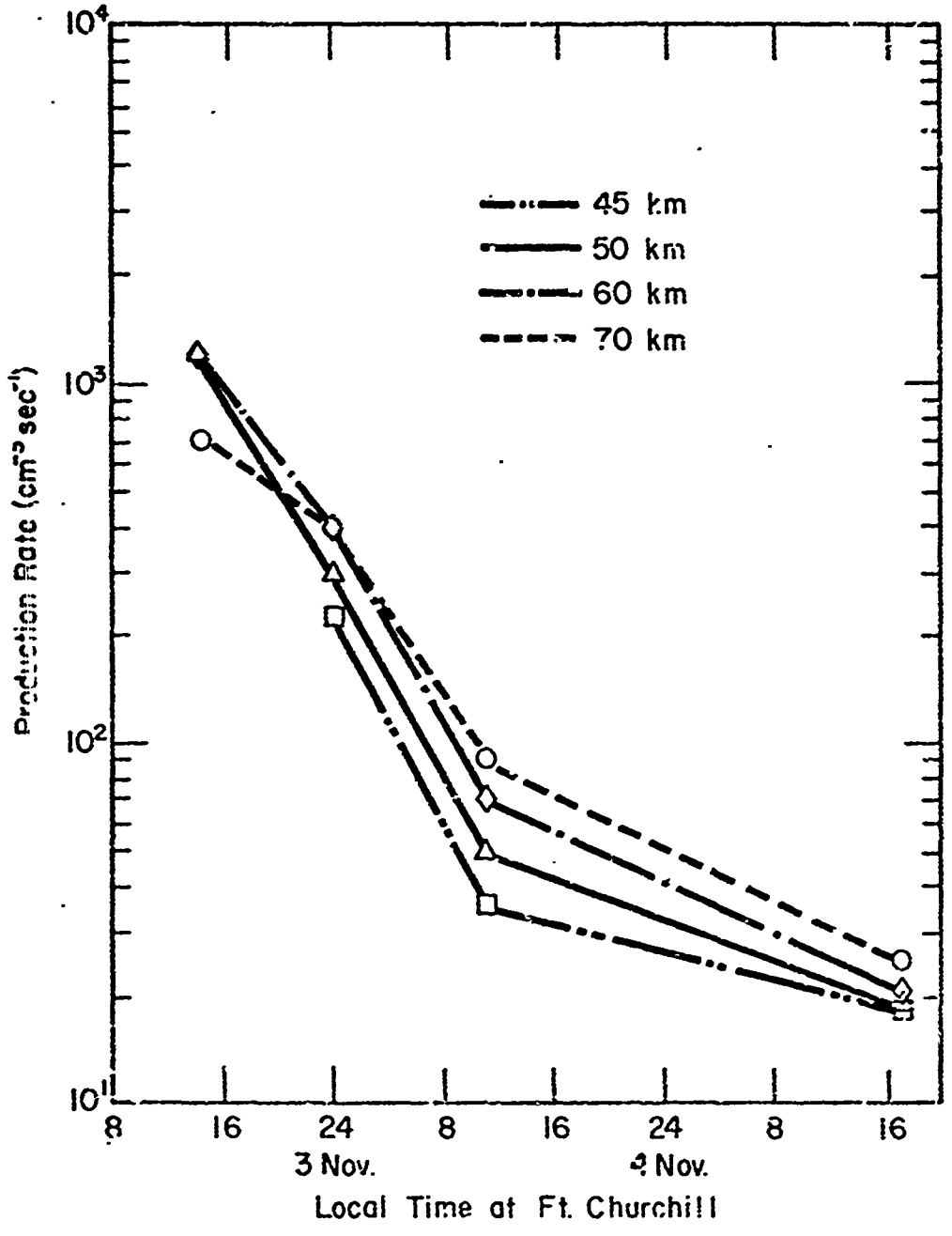

Figure 4-2. Production rates during the November 2, 1969 PCA from extrapolation of the preliminary rates of Swider and Gardner (1972).

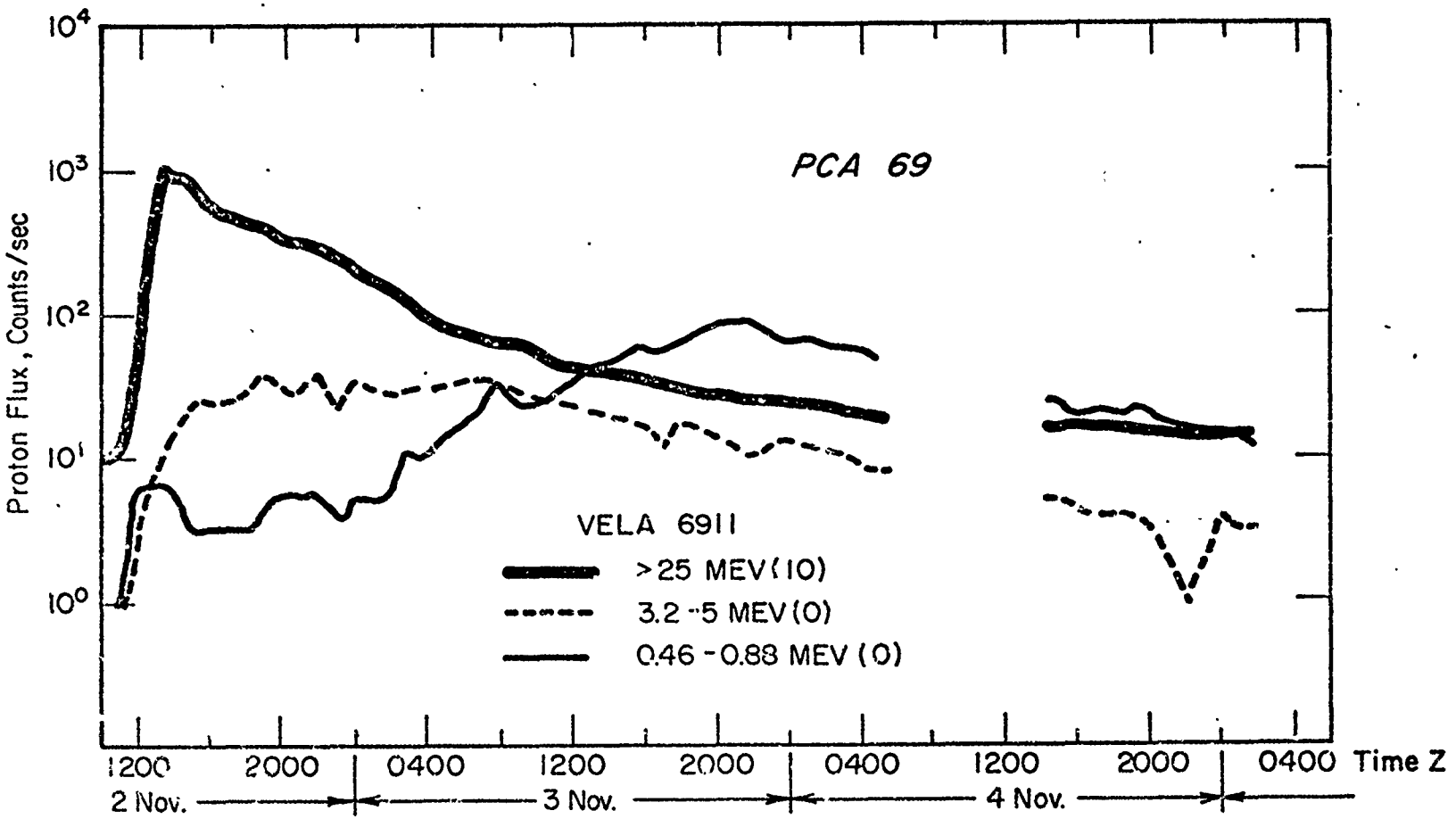

Figure 4-3. Proton flux variations during the November 2, 1969 PCA (Ulwick; 1971/courtesy of S. Singer, Los Alamos Scientific Laboratories).

Using the extrapolated rates, α_{eff} for each of the four Arcas flights was calculated and appears in Figure 4-4. The estimated accuracy of α_{eff} is about a factor of two, based upon the known electron density errors and an assumed $\pm$ 25% error in the calculated production rates.

The plot of α_{eff} for the Arcas results shows that the electron loss mechanisms decrease with decreasing zenith angle. Figure 4-4 also shows a comparison of α_{eff} with the results of others, taken from a compilation by Potemra et al (1970) in their study of the PCA events of 1967 using very low frequency propagation data. It is noted that α_{eff} during the H-6 daytime flight and the H-2 nighttime flight compare reasonably well with the daytime and nighttime results of Potemra et al. Between around 58 and 63 km the nighttime value of α_{eff} was around 10^3 - 10^4 greater than the daytime value.

4.2.1 Interpretation of Nighttime Results

Swider et al (1971) interpreted nighttime effective electron loss coefficient results obtained during a PCA that occurred on November 18, 1968. They found that the electron density behaves according to $N \simeq Q/L(A)$, $Z < 75$ km, where L(A) is the electron loss rate due to attachment by the processes

$$e + O_2 + O_2 \rightarrow O_2^- + O_2 \quad \left[1.4 \times 10^{-29}\left(\frac{300}{T}\right)\exp\left(\frac{-600}{T}\right)\right]$$

$$e + O_2 + N_2 \rightarrow O_2^- + N_2 \quad \left[10^{-31}\ \text{cm}^6\text{-sec}^{-1}\right]$$

Accordingly, calculations of α_{eff} using Swider et al's L(A) and the estimated Q corresponding approximately to the time of rocket flight H-2 (Figure 4-1, Curve 3 Nov. 69, 0005 CST) gives the results shown in Figure 4-5. This calculated α_{eff} compares very well with the nighttime values obtained from $\alpha_{eff} = Q/N^2$ and indicates, as noted by Swider et al, that electron detachment is inoperative at night and that the primary electron loss mechanism is three-body attachment to molecular oxygen.

4.3 Calculation of the Negative Ion Density to Electron Density Ratio

Hale et al (1971) deduced the positive ion densities shown in Figure 4-6 from the Arcas blunt probe measurements. Comparison of Hale's positive ion densities and electron densities shows that $N_+ \gg N$. Therefore, the neutrality condition, $N_+ = N_- + N$, indicates that the negative and positive ion densities are practically equal. The parameter λ can then be calculated accordingly:

$$\lambda = \frac{N_-}{N} \approx \frac{N_+}{N} \qquad (4.7)$$

Results for those flights where data coincide (H-3 and H-4) are shown in Figure 4-7. Again the greater effectiveness of apparent electron detachment at lower altitudes with change in solar zenith angle is observed by noting the increase in the difference between the λ of H-4 and that of H-3 below 58 km; above this height the λ's appear

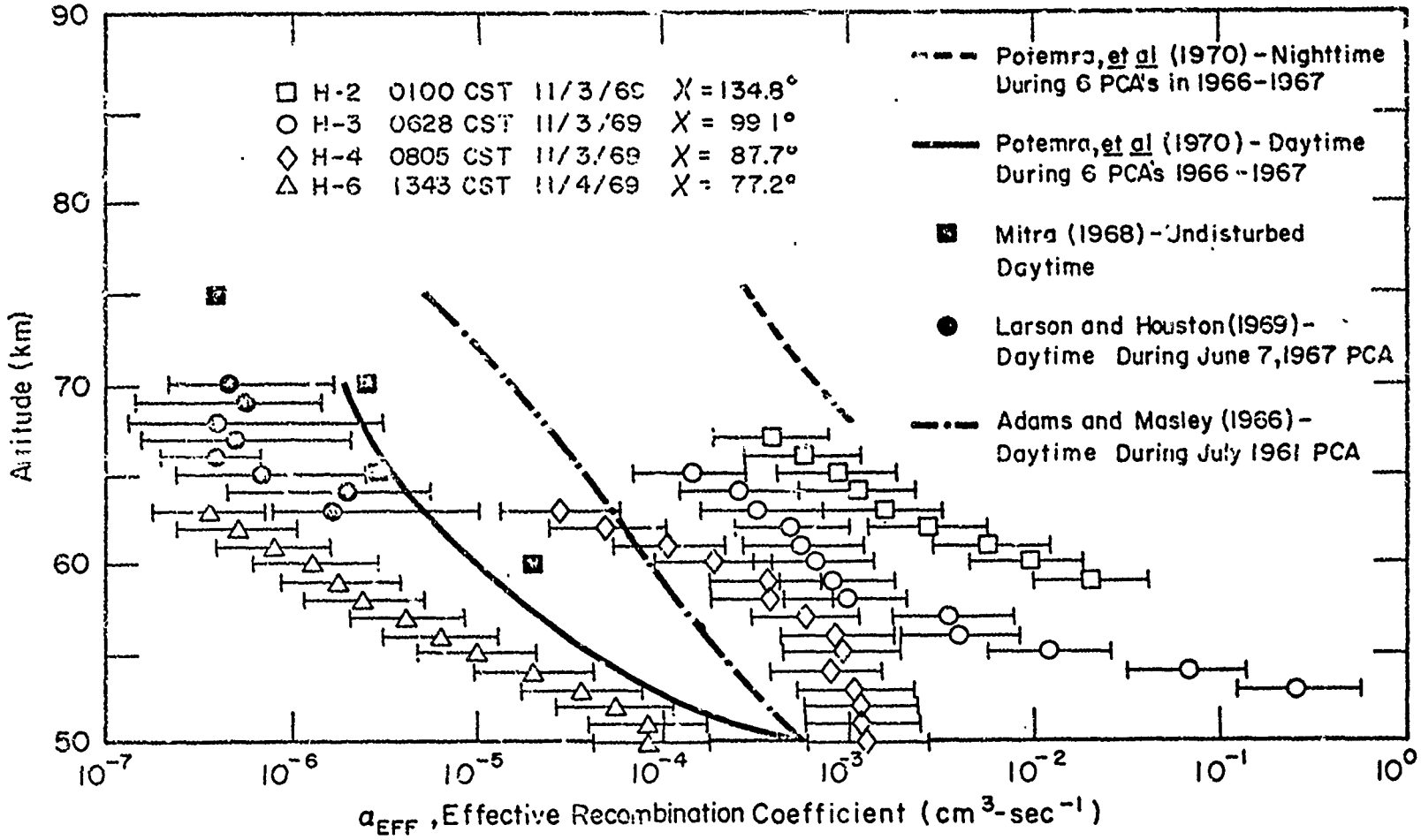

Figure 4-4. Comparison of the effective recombination coefficients from the Arcas electron density profiles with others.

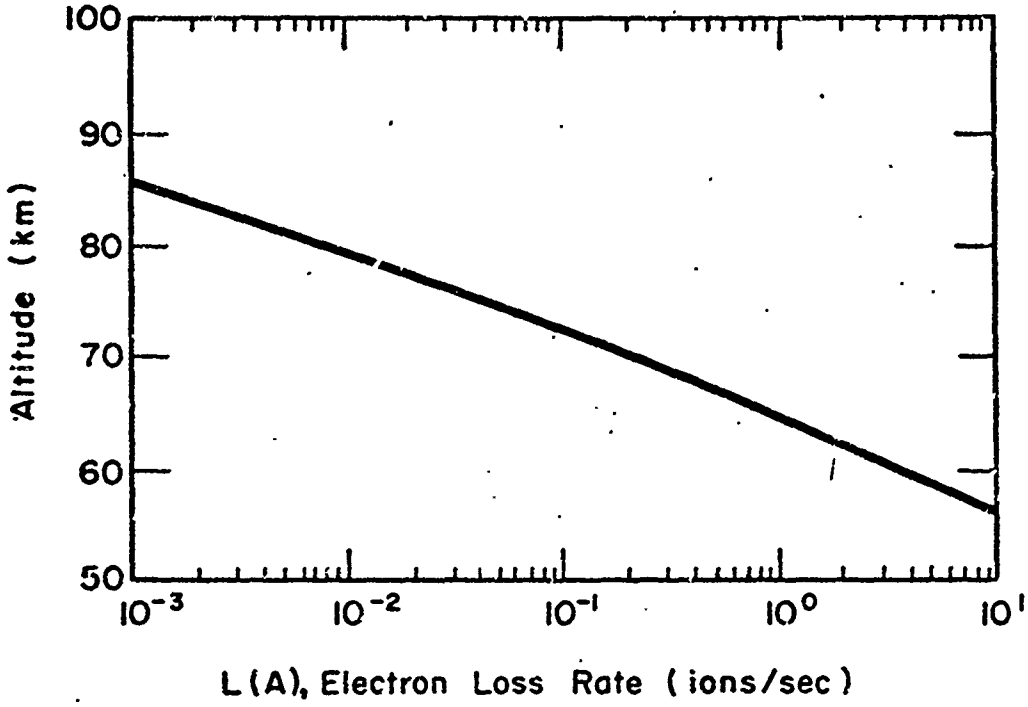

Figure 4-5 a. Electron loss coefficient, L(A), after Swider et al (1971).

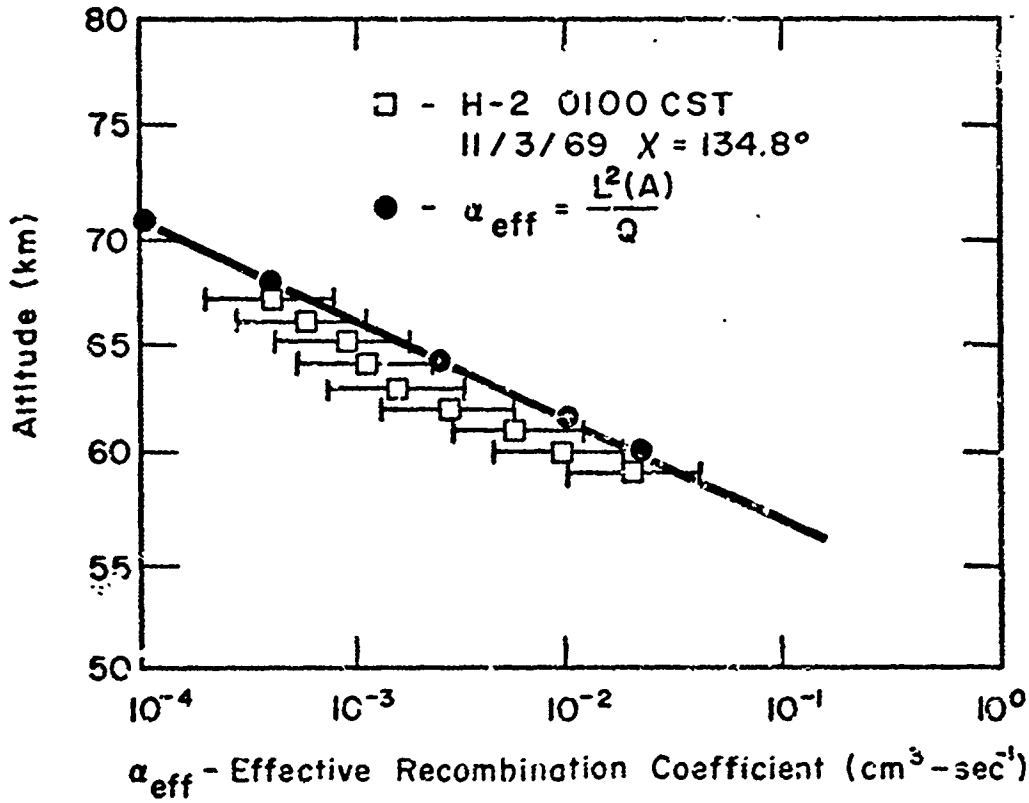

Figure 4-5 b. Comparison of nighttime $\alpha_{eff} = \frac{Q}{N^2}$ from H-2 with $\alpha_{eff} = \frac{L^2(A)}{Q}$, L(A) given in Fig. 4-5 a and Q given in Fig. 4-1.

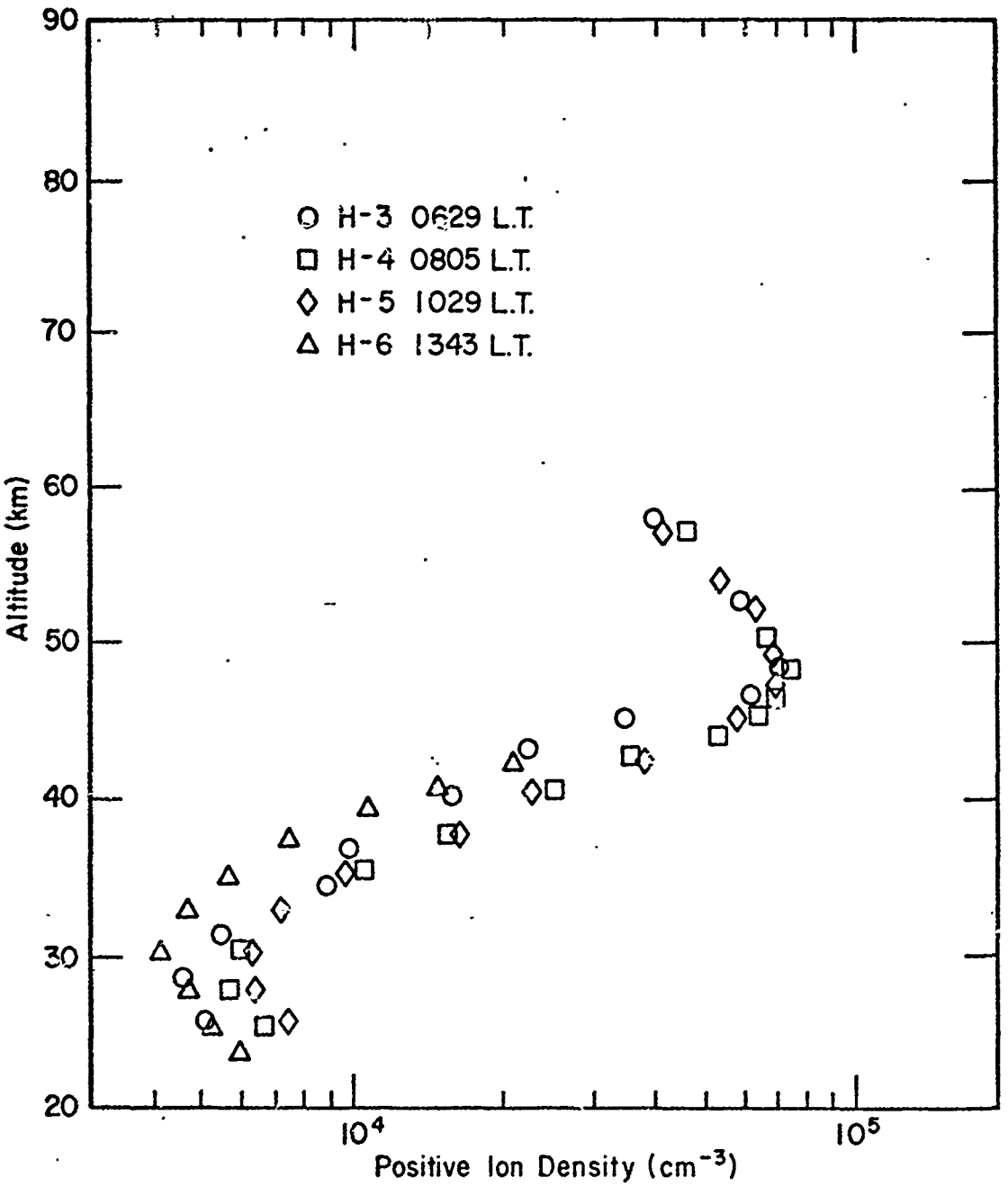

Figure 4.6. Positive ion density data for Ft. Churchill, Canada from Hale, et al (1971).

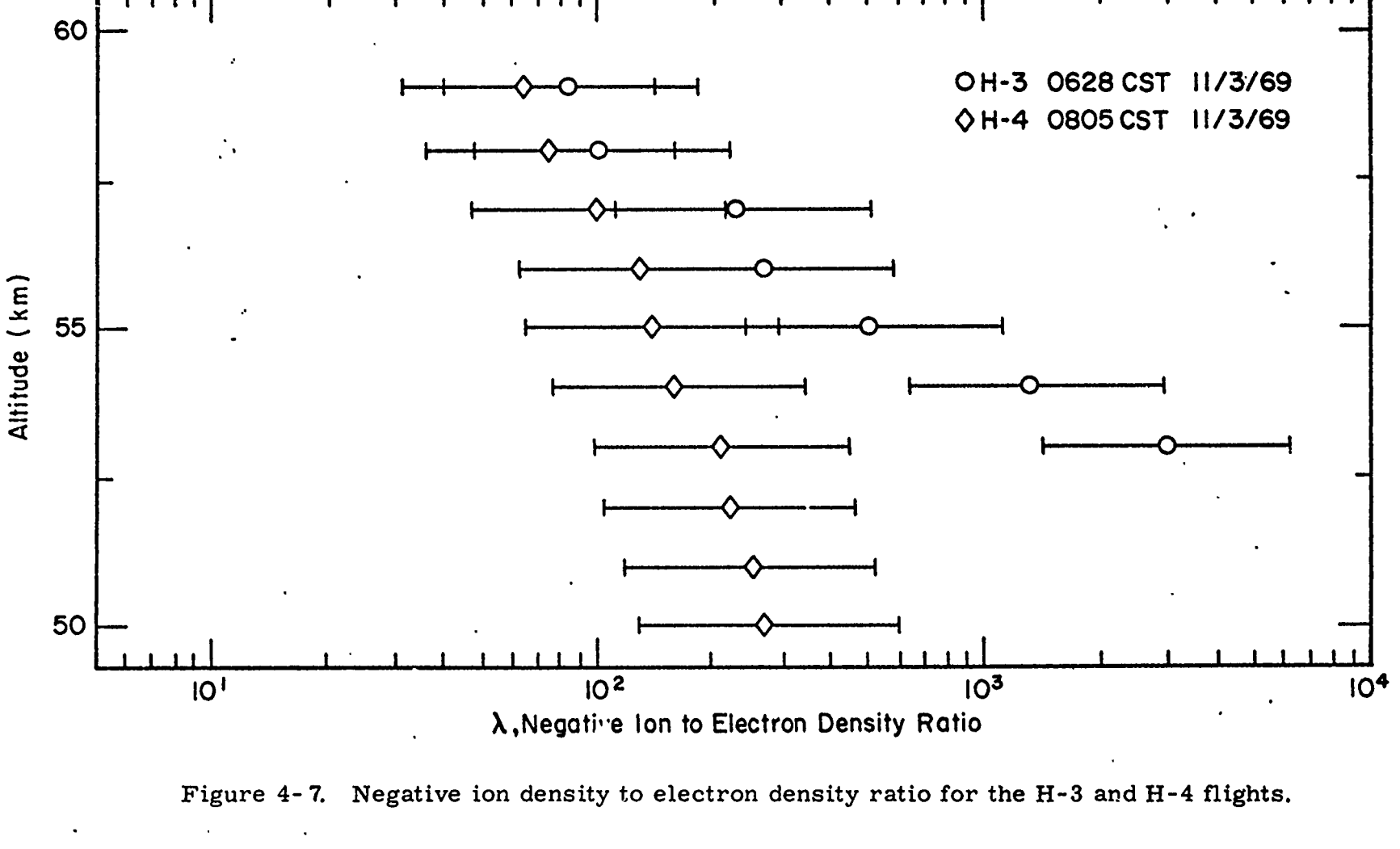

Figure 4-7. Negative ion density to electron density ratio for the H-3 and H-4 flights.

to be nearly equal. These significant differences in the λ's below 56 km again demonstrate the sensitivity of this part of the D region to solar radiation during the sunrise period.

4.4 Estimates of the Ionic Neutralization and the Dissociative Recombination Coefficient

The positive ion equation, Equation 4.3, under quasi-equilibrium conditions may be written as

$$NN_+ = \frac{Q}{\alpha_d + \alpha_i \lambda} \tag{4.8}$$

At night and at low altitudes the electron recombination process is often assumed to be small, that is $\alpha_d \ll \alpha_i \lambda$. Assuming that this is valid and that $N_+ \approx N_-$, then

$$N_+ = \left[\frac{Q}{\alpha_i}\right]^{1/2} \tag{4.9}$$

or

$$\alpha_i = \frac{Q}{N_+^2} \tag{4.10}$$

From the data of Swider and Gardner (1972) and Hale et al (1971), α_i can be estimated from Equation 4.10. The resultant values for α_i are plotted in Figure 4-8. α_i ranges between around 10^{-8} to 10^{-7} cm^3-sec^{-1} and may be associated with two-body ion-ion neutralization involving water cluster ions. Examples of such reactions thought to be important in the low D region include (Swider and Keneshea; 1972):

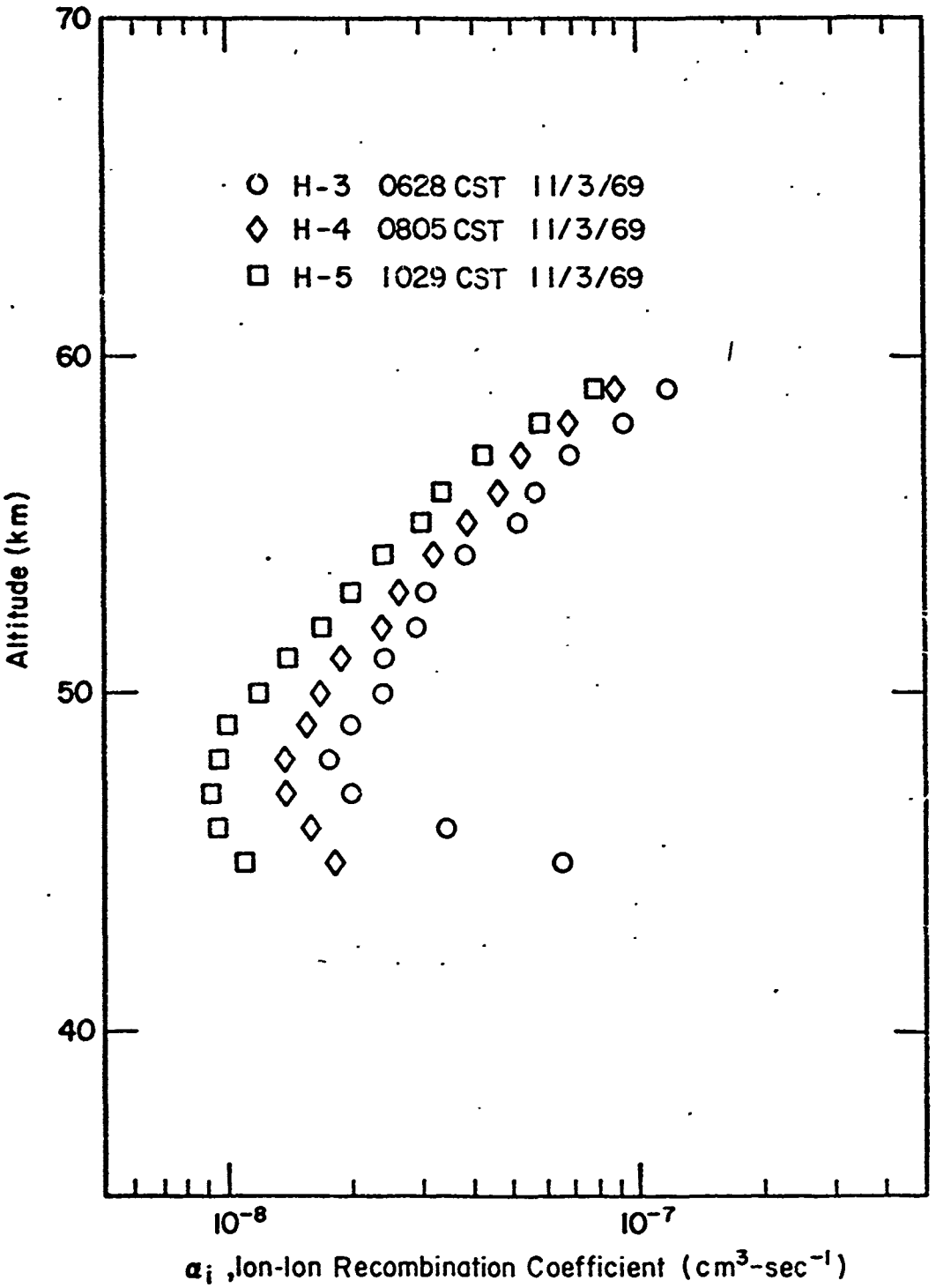

Figure 4-8. Approximate calculation of the ion-ion neutralization coefficient ($\approx Q/N_\perp^2$) for the H-3, H-4, and H-5 Arcas rocket flights.

$$H_3O^+ + X^- \rightarrow H_2O + \ldots.$$

$$H_3O^+ \cdot H_2O + X^- \rightarrow 2H_2O + \ldots.$$

$$H_3O^+ \cdot 2H_2O + X^- \rightarrow 3H_2O + \ldots.$$

$$H_3O^+ \cdot 3H_2O + X^- \rightarrow 4H_2O + \ldots.$$

$$H_3O^+ \cdot 4H_2O + X^- \rightarrow 5H_2O + \ldots.$$

$$H_3O^+ \cdot OH + X^- \rightarrow 2H_2O + \ldots..$$

where X^- represents non-cluster negative ions thought to be present in the D region, such as O^-, O_2^-, O_3^-, O_4^-, NO_2^-, NO_3^-, $OONO^-$, CO_3^-, CO_4^-. The rate constants for these reactions have not yet been measured in the laboratory, but are expected to range in the neighborhood between about 1×10^{-8} to 10^{-7} $cm^3 s^{-1}$ with a rate that decreases with increasing hydration (Niles, 1973).

The curves show that α_i reaches a minimum around 48 km. The increase of α_i with decreasing altitude below this height is consistent with expectations, since α_i consists of two basic neutralization processes: two-body and three-body, i.e.,

$$\alpha_i = \alpha_{i2} + \alpha_{i3} \qquad (4.11)$$

where α_{i2} and α_{i3} are the two-body and three-body neutralization coefficients respectively.

The variation of α_i with height depends on whether two-body or three-body recombination dominates and on the ionic species. Under normal atmospheric conditions, the pressure dependence of the three-

body process should dominate at altitudes where the pressure exceeds 1 mm of Hg (Hasted; 1964). Using the CIRA 1965 atmospheric model, the altitude where this occurs would be around 48 km. Thus, we would expect α_i to be pressure dependent below this altitude ($\alpha_i \approx \alpha_{i3}$), increasing at an exponential rate, probably with the local scale height. Above 48 km one would expect two-body recombination to be the dominate ion-ion neutralization process ($\alpha_i \approx \alpha_{i2}$). Further, if the ionic constituents remain the same above this altitude, we would expect α_i to be approximately constant, independent of pressure and thus altitude. The results of Figure 4-8 show that α_i increases with altitude above 48 km. Given the results of Narcisi (1971) who measured positive and negative ion mass densities during the PCA, this may be interpreted in several ways; either ion-ion neutralization is dominated by a combination of cluster-cluster and non-cluster-cluster neutralization processes that might change with height as the ionic constituents change, or Equation 4.10 is invalid and electron dissociative recombination is significant. With available data this first hypothesis cannot be adequately tested. However, a chemistry scheme is presented in the next section to demonstrate a method of analysis and show how minor constituents can play an important role in the actual ion-ion neutralization in the region.

If 48 km is considered as the height where $\alpha_{i3} \approx \alpha_{i2}$, then from Figure 4-8 and Equation 4.11 $\alpha_{i2} \approx 5\text{-}8 \times 10^{-9}$ $cm^3 s^{-1}$. This would

imply that, if cluster ions dominate entirely, the rate for cluster-cluster reactions is of this order. We note that this rate has not yet been measured for any expected reactions in the laboratory and is a consideration which would require further study. It is also noted that this lower estimate for α_{i2} is about an order of magnitude less than the estimated rates used by Swider and Keneshea(1972) in their computations, simulating D region behavior during PCA events.

4.4.1 Minor Constituents in the Ion-Ion Neutralization Process

Although the calculated α_i from ionospheric parameters measured during the PCA between 50-60 km is of the order of expected cluster-non-cluster rates, the height variation requires explanation. Clearly, changes in ionic constituents are possible. This possibility will now be considered.

To consider the role played by the various ionic species in the ion-ion neutralization process, the total negative and positive ions are each decomposed into total water cluster and non-water cluster components; that is

$$N_- = N_{c_-} + N_{n_-}$$

and

$$N_+ = N_{c_+} + N_{n_+}$$

where N_{c_-} and N_{c_+} are the total negative and positive water cluster ions respectively; N_{n_-} and N_{n_+}, the total negative and positive non-

water cluster ions respectively. Under these circumstances the quasi-equilibrium positive ion continuity equation becomes

$$Q - \alpha_{i_{c_-c_+}} N_{c_-} N_{c_+} - \alpha_{i_{c_-n_+}} N_{c_-} N_{n_+} - \alpha_{i_{c_+n_-}} N_{c_+} N_{n_-} - \alpha_{i_{n_-n_+}} N_{n_-} N_{n_+} = 0 \qquad (4.12)$$

where the sub-scripts of α_i denote the possible combination of cluster and non-cluster ions for which ion-ion neutralization may occur; for example, $\alpha_{i_{c_-c_+}}$ denotes the coefficient associated with the neutralization of a negative cluster with a positive cluster ion.

Letting $k_- = \frac{N_{n-}}{N_-}$ and $k_+ = \frac{N_{n_+}}{N_+}$ denote the fraction of the total negative and positive ions which are non-clusters respectively, we may rewrite Equation 4.12 as

$$Q - \left[\alpha_{i_{c_-c_+}} (1 - k_-)(1-k_+) + \alpha_{i_{c_-n_+}} (1-k_-) k_+ + \alpha_{i_{c_+n_-}} (1-k_+)k_- + \alpha_{i_{n_-n_+}} k_+k_- \right] N_-N_+ = 0$$

Hence, we have

$$\alpha_i = \alpha_{i_{c_-c_+}} (1-k_-)(1-k_+) + \alpha_{i_{c_-n_+}} (1-k_-)k_+ + \alpha_{i_{c_+n_-}} (1-k_+)k_- + \alpha_{i_{n_-n_+}} k_+k_- \qquad (4.13)$$

α_i, so written, reveals the relative importance that each of the ionic species plays in the neutralization process.

In particular, if the non-cluster ions are minor constituents, i.e. k_+, $k_- \lesssim 0.1$ and $\alpha_{i_{n_-n_+}} \approx 10^{-7}$, then the last term in Equation 4.13 must be negligible, considering the α_i obtained previously in Figure 4-8. Based on the assumption that k_+, $k_- \lesssim 0.1$, then

$$0.81 < (1-k_-)(1-k_+) < 1,$$

$$0 < (1-k_+)k_- < 0.09,$$

$$0 < (1-k_-)k_+ < 0.09.$$

From Figure 4-7 we may estimate the magnitude of $\alpha_{i_{c_-n_+}}$ and $\alpha_{i_{c_+n_-}}$ to be about 10^{-8} - 10^{-7} $cm^3 s^{-1}$; from the previous section $\alpha_{i_{c_-c_+}}$ was estimated to be about 5×10^{-9} - 10^{-8} $cm^3 s^{-1}$. Using these estimates, we can see that the first three terms in Equation 4.13 can be of the same order of magnitude, and as a result the effective ion-ion neutralization would be dependent on the fractional concentration of cluster and non-cluster ions. These results require further study and test as more specific data on cluster ions and their chemistry become available.

4.4.2 Electron Dissociative Recombination Effects

In Section 4.4 we hypothesized that if the chemistry is the same in the height region of interest, then a possible explanation for the increase in α_i with height is that dissociative recombination is important and must be considered in the positive ion continuity equation.

To consider such a possibility, the values of the dissociative recombination coefficient required to balance the quasi-equilibrium positive ion equation, using the Arcas electron and charged particle densities and production rates, were calculated for various assumed constant ion-ion neutralization coefficients. The curves are shown in Figures 4-9 and 4-10 for H-3 and H-4 respectively.

If α_d is significant enough to be considered in balancing the positive ion equation and if the chemistry is relatively constant in the region of interest, then reasonable values for α_d and α_i would be those combinations which would yield constants. Given the errors in the data, such a region is shown blocked in Figures 4-9 and 4-10. For H-3, the region is above about 55 km with α_d and α_i of the order of $4\text{-}9\times10^{-6}$ cm^3 s^{-1} and $3\text{-}4\times10^{-8}$ cm^3 s^{-1} respectively. For H-4 the region is above 54 km with α_d and α_i of the order of $3\text{-}5\times10^{-6}$ cm^3 s^{-1} and $1\text{-}2\times10^{-8}$ cm^3 s^{-1} respectively. It is noted that these values of α_d are consistent with those considered applicable for this region for a complex water cluster ion chemistry (Aiken et al; 1972). The known possible positive cluster ion-electron dissociative recombination reactions applicable to this portion of the D region are given below for comparison with the deduced α_d's of this section (Leu et al; 1973).

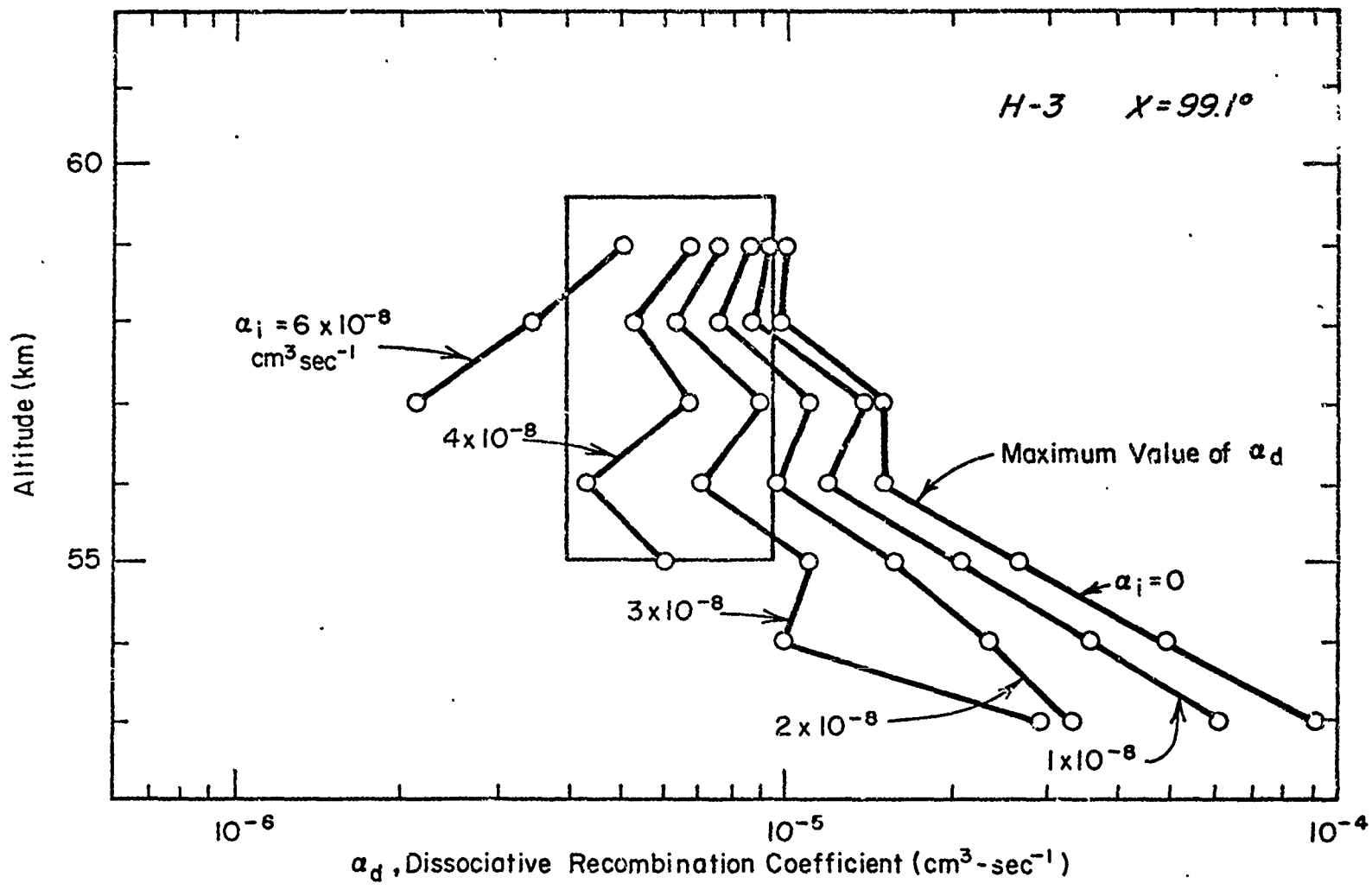

Figure 4-9. Possible combinations of α_d and α_i necessary to balance the positive ion equation using the H-3 Arcas data.

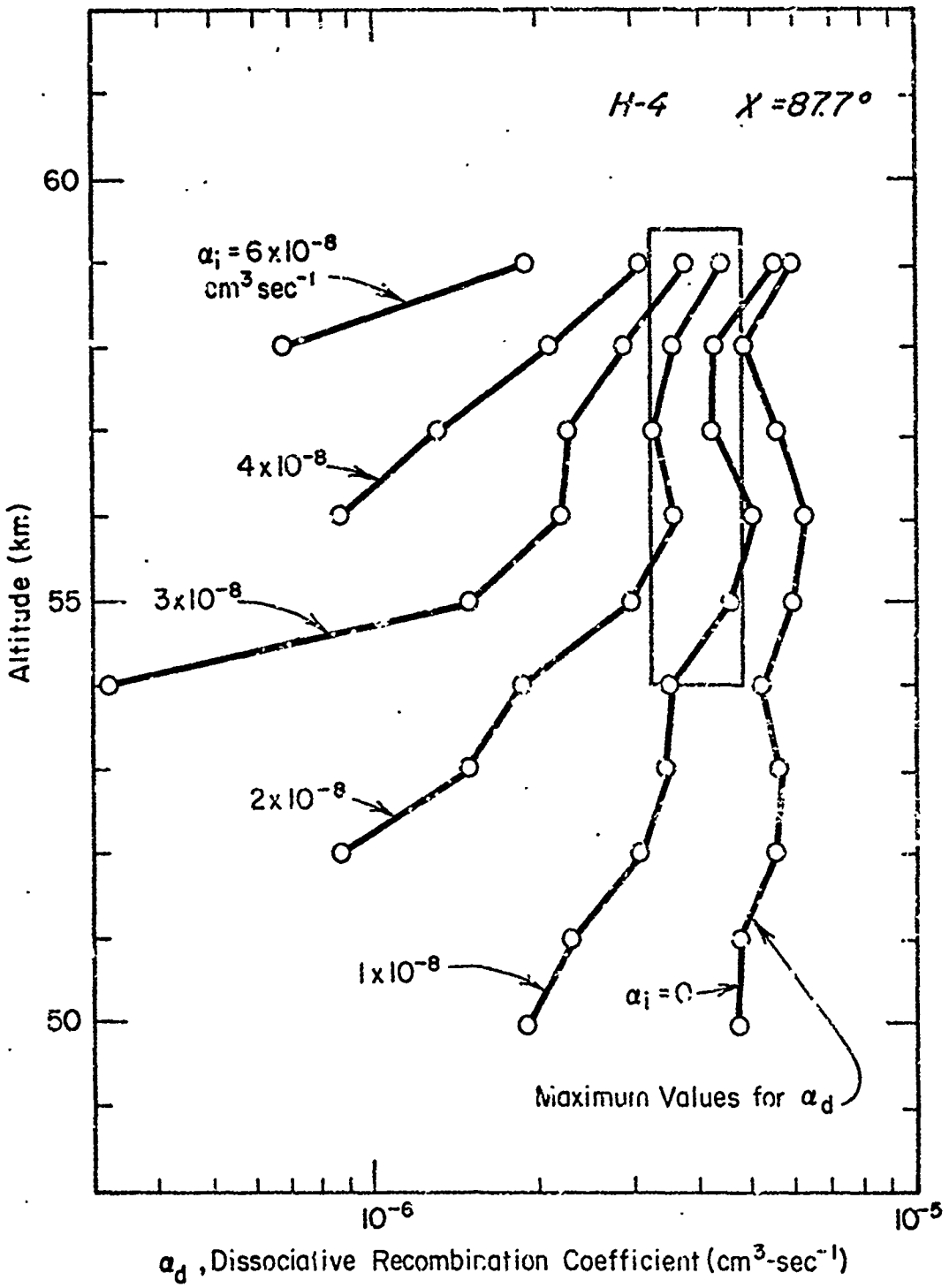

Figure 4-10. Possible combinations of α_d and α_i necessary to balance the positive ion equation using the H-4 Arcas data.

$H_3O^+ + e \rightarrow H + H_2O$ ($1.0 \pm 0.2 \times 10^{-6}$ cm^3 s^{-1} @ 540°K)

$H_3O^+ \cdot H_2O + e \rightarrow H + 2H_2O$ ($2.2 \pm 0.4 \times 10^{-6}$ cm^3 s^{-1} @ 415°K)

$H_3O^+ \cdot 2H_2O + e \rightarrow H + 3H_2O$ ($3.8 \pm 0.6 \times 10^{-6}$ cm^3 s^{-1} @ 300°K)

$H_3O^+ \cdot 3H_2O + e \rightarrow H + 4H_2O$ ($4.9 \pm 0.8 \times 10^{-6}$ cm^3 s^{-1} @ 300°K)

$H_3O^+ \cdot 4H_2O + e \rightarrow H + 5H_2O$ ($6.0 \pm 1.2 \times 10^{-6}$ cm^3 s^{-1} @ 205°K)

$H_3O^+ \cdot 5H_2O + e \rightarrow H + 6H_2O$ ($7.5 \pm 1.5 \times 10^{-6}$ cm^3 s^{-1} @ 205°K)

$H_3O^+ \cdot 6H_2O + e \rightarrow H + 7H_2O$ ($\leq 10^{-5}$ cm^3 s^{-1} @ 205°K)

Other examples of possibly important, but still unmeasured, recombination reactions involving hydrated ions include:

$$O_2^+ \cdot H_2O + e \rightarrow O_2 + H_2O$$

$$H_3O^+ \cdot OH + e \rightarrow H_2O + H_2O$$

$$NO^+ \cdot H_2O + e \rightarrow NO + H_2O$$

$$NO^+ \cdot 2H_2O + e \rightarrow NO + 2H_2O$$

$$NO^+ \cdot 3H_2O + e \rightarrow NO + 3H_2O$$

Further consideration of Figures 4-9 and 4-10 indicates significant differences for the requirement of α_d between H-3 and H-4. Below 56 km and for constant α_i, the results of H-3 show that $10^{-5} \lesssim \alpha_d \lesssim 10^{-4}$ cm^3 s^{-1} is required and that α_d increases with decreasing height; for H-4, $3 \times 10^{-7} \lesssim \alpha_d \lesssim 6 \times 10^{-6}$ cm^3 s^{-1} is required and α_d decreases with decreasing height.

The large differences between these two results can possibly be attributed to the D region chemistry during the sunrise period. Reid

(1961) showed from measured riometer observations that for zenith angles greater than approximately 99^{o} the D region is at its nighttime quasi-equilibrium state, and for angles less than approximately 87^{o} the D region is at its daytime state. Hence, the results for H-3 ($\chi = 99.1^{o}$) depicts the nighttime D region chemistry; while H-4 ($\chi = 87.7^{o}$), the daytime chemistry. From this one can suggest that, since rates for α_d are usually greater than 10^{-6} cm^3 s^{-1} and since there is a tendency for the rates to increase with an increase in the mass of positive water cluster ion, the nighttime chemistry as evident by the results of H-3 is very much dominated by heavy water cluster ions, while during the day the water cluster ions are either lighter in mass or become less of an influence in the D region than at night. This suggestion is offered as an explanation for the large differences between the α_d's for the H-3 and the H-4 results at the lower heights; it is further noted that such a suggestion is open to question, but as further data become available we may be better able to support or discredit it.

CHAPTER V

CONCLUSIONS

Electron densities were deduced from the H-2, H-3, H-4 and H-6 Arcas propagation experiments conducted during the November 2, 1969 PCA event. The Arcas results compare reasonably well with the electron density profiles obtained by Dean (1971).

Using available production rates and charged particle densities, the ionospheric parameters, the effective recombination coefficient and the negative ion density to electron density ratio were calculated. These calculations suggested an increasing importance of electron detachment during the night-sunrise period with decreasing height. The nighttime results from rocket H-2 for the effective electron loss coefficient compared well with other measurements of Swider et al (1971) who showed that electron detachment is inoperative at night and that three-body attachment to molecular oxygen is most likely the primary loss mechanism for electrons below around 75 km.

Estimates of the ionic recombination coefficient, α_i, were made based on the assumption that electron recombination was insignificant in the altitude range of about 45 to 60 km. The values of α_i were found to lie within a range which is expected to apply to water cluster

ion chemistry. The increase in α_i below 48 km may be evidence for α_i being dependent on pressure, thereby introducing the possibility that three-body neutralization processes may begin to dominate two-body processes below this height. Possible explanations for the increase of α_i with height above 48 km were also given.

One explanation was the possible dominance of water cluster ions in the neutralization processes which might change with height. A chemical scheme which considered the possible two-body neutralization processes between cluster and non-cluster ions revealed the complex makeup of the overall effective ion-ion neutralization coefficient which can possibly explain the observed increase in α_i.

Another explanation was that dissociative recombination is important in the low D region. A consideration of this possibility revealed that, if electron recombination is important, its rate coefficient would be of an order consistent with reactions involving cluster ions. Further, it was suggested that at night the water cluster ions in the low D region would be heavier than those involved in the daytime chemistry.

These discussions of the electron density results were based primarily on available data of electron production rates and ion densities. As more data concerning the November 2, 1969 PCA becomes available, the electron densities should contribute to further understanding of D region chemistry during disturbed polar cap

conditions.

In addition, the electron density results should prove particularly useful in testing the validity of detailed computer models that include the effects of all known reactions, production rates, and transport effects in the low D region.

BIBLIOGRAPHY

Adams, G. W. and A. J. Masley (1966), "Theoretical Study of Cosmic Noise Absorption Due to Solar Cosmic Radiation," Planetary and Space Science, 14, 277-290.

Adams, G. W. and L. R. Megill (1967), "A Two-Ion D-Region Model For Polar Cap Absorption Events," Planetary and Space Science, 15, 1111-1130.

Aiken, A. C., R. A. Goldsberg, Y. V. Somayajulu, and M. B. Avadhanulu (1972), "Electron and Positive Ion Density Altitude Distributions in the Equatorial D-Region," Journal of Atmospheric and Terrestrial Physics, 34, 1483-1494.

Bailey, D. K. (1959), "Abnormal Ionization in the Lower Ionosphere Associated with Cosmic-Ray Flux Enhancements," Proceedings of the Institute of Radio Engineers, 47, 255-266.

Bailey, D. K. (1964), "Polar Cap Absorption," Planetary and Space Science, 12, 495-541.

Budden, K. G. (1955), "The Numerical Solution of Differential Equations Governing Reflexion of Long Radiowaves from the Ionosphere," Proceedings of the Royal Society A (London), 227, 516-537.

Budden, K. G. (1964), Lectures on Magnetoionic Theory, (Gordon and Breach Science Publishers. New York, 1964).

Budden, K. G. (1966), Radio Waves in the Ionosphere, (Cambridge University Press, Cambridge, 1966).

Bowhill, S. A. and E. A. Mechtly (1961), "An Ionosphere Electron Density Experiment Particularly Suited for Small Rockets," in Space Research II, ed. by H. C. Van de Hulst, C. de Jager and A. F. Moore, (North-Holland Publishing Co., Amsterdam, 1961), 1208-1214.

CIRA 1965, COSPAR International Reference Atmosphere, (North-Holland Publishing Company, Amsterdam, 1965).

Clemmow, P. C. and J. Heading (1954), "Coupled Forms of the Differential Equations Governing Radio Propagation in the Ionosphere," Proceedings of the Cambridge Philosophical Society, 50, Part 2, 319-333.

Danilov, A. D. (1970), Chemistry of the Ionosphere, (Plenum Press, New York, 1970).

Dean, W. A. (1971), "Electron Density Profiles for the 1969 PCA Event," a paper presented at the COSPAR Symposium on November 1969 Solar Particle Event, June 16-18, 1971, Boston College, Chestnut Hill, Massachusetts, to be published in Symposium Proceedings.

Hale, L. C. (1967), "Parameters of the Lower Ionosphere at Night Deduced from Parachute Borne Blunt Probe Measurements," in Space Research VII, ed. by R. L. Smith-Rose, (North-Holland Publishing Company. Amsterdam, 1967), 140-151.

Hale, L. C., D. P. Hoult, and D. C. Baker (1968), "Summary of Blunt Probe Theory and Experimental Results," in Space Research VIII, ed. by A. P. Mitra, L. G. Jacchia, and W. S. Newman, (North-Holland Publishing Company, Amsterdam, 1968), 320-331.

Hale, L. C. and T. A. Seliga (1970), "Preliminary Assessment of Arcas Blunt Probe and Propagation Data During a PCA," Proceedings of Meeting on Operation PCA 69, Air Force Cambridge Research Laboratory Report No. 110, 101-106.

Hale, L. C., J. R. Mentzer, and L. C. Nickell (1971), "Blunt Probe Measurements During a PCA Event," a paper presented at the COSPAR Symposium on November 1969 Solar Particle Event, June 16-18, 1971, Boston College, Chestnut Hill, Massachusetts, to be published in Symposium Proceedings.

Hall, J. E. (1964), "Electron Densities in the D region from Rocket Measurements," Electron Density Distributions in Ionosphere and Exosphere, ed. by E. Trane, (North-Holland Publishing Co., Amsterdam, 1964), 11-12.

Hasted, J. B. (1964), Physics of Atomic Collisions, (Butterworth and Co., Ltd., London, 1964), 270-274.

Holt, O. (1968), "Characteristics of Polar Cap Absorption," in Ionospheric Radio Communications, ed. by Kristen Folkestad, (Plenum Press, New York, 1968), 33-45.

Larson, L. E. and R. E. Houston, Jr. (1969), "A Measurement of the Effective Recombination Coefficient in the Lower Ionosphere," Journal of Geophysical Research, 74, 2402-2406.

Leu, M. T., M. A. Biondi and R. Johnsen (1973), "Measurements of the Recombination of Electrons with $H_3O^+ \cdot (H_2O)_n$ - Series Ions," Phys. Rev. A, 7, 292-298.

Melrose, B. T. and L. C. Hale (1970), private communications.

Mitra, A. P. (1968), "A Review of D-region Processes in Non-Polar Latitudes," Journal of Atmospheric and Terrestrial Physics, 42, 2048-2062.

Narcisi, R. S., A. D. Bailey, L. Della Lucca, C. Sherman, and D. M. Thomas (1971), "Mass Spectrometric Measurements of Negative Ions in the D- and Lower E-Regions," Journal of Atmospheric and Terrestrial Physics, 33, 1147-1159.

Niles, F. E. (1973), personal communications.

Phelps, A. V. and J. L. Pack (1959), "Electron Collision Frequencies in Nitrogen and in the Lower Ionosphere," Physical Review Letters, 3, 340-342.

Pitteway, M. L. V. (1965), "The Numerical Calculation of Wave-Fields, Reflexion Coefficients and Polarizations of Long Radio Waves in the Lower Ionosphere." I, Transactions of the Royal Society A (London), 257, 219-241.

Potemra, T. A., A. J. Zmuda, B. W. Shaw, and C. R. Haave (1970), "VLF Phase Disturbances, HF Absorption, and Solar Protons in the PCA Events of 1967," Radio Science, 5, 1137-1145.

Reid, G. C. and C. Collins (1959), "Observations of Abnormal VHF Radio Wave Absorption at Medium and High Latitudes," Journal of Atmospheric and Terrestrial Physics, 14, 63-81.

Reid, G. C. and H. Leinbach (1961), "Morphology and Interpretation of the Great Polar Cap Absorption Events of May and July, 1959," Journal of Atmospheric and Terrestrial Physics, 23, 216-228.

Reid, G. C. (1961), "A Study of the Enhanced Ionization Produced by Solar Protons during a Polar Cap Absorption Event," Journal of Geophysical Research, 66, 4071-4085.

Reid, G. C. (1965), "Solar Cosmic Rays in Ionosphere," in Physics of the Earth's Upper Atmosphere, ed. by C. O. Hines, I. Paghis, T. R. Hartz, and J. A. Fejer, (Prentice-Hall, Inc., Englewood Cliffs, New Jersey, 1965), 245-270.

Seliga, T.A. (1966), "Numerical Full Wave Solution Techniques for the Calculation of Low Frequency Plane Wave Fields in the Ionosphere," Journal of the Institute of Telecommunication Engineers, 12, 198-213.

Seliga, T.A. (1968), "Analysis and Results of Low-Frequency CW Rocket Propagation Experiments in the D Region," Journal of Geophysical Research, 73, 6783-6794.

Sen, H.K. and A.A. Wyler (1960), "On the Generalization of the Appleton-Hartree Magnetoionic Formulas, "Journal of Geophysical Research, 65, 3931-3949.

Swider, W., R.S. Narcisi, T.J. Keneshea and J.C. Ulwick (1971), "Electron Loss during a Nighttime PCA Event," Journal of Geophysical Research, 76, 4691-4694.

Swider, W. and M.E. Gardner (1972), private communications.

Swider, W. and T.J. Keneshea (1972), " Diurnal Variations in the D Region During PCA Events," Air Force Cambridge Research Laboratories Report AFCRL-72-0474, 589-636.

Ulwick, J.C. (1971), "Operation PCA 69 -- An Investigation of the Solar Particle Event of 2 November 1969," in Space Research XI, ed. by K. Ya Kondratyev, M.J. Rycroft, and C. Sagan, (Akademie-Verlag, New York, 1971), 1181-1187.

Whitten, R.C. and I.G. Poppoff (1965), Physics of the Lower Ionosphere, (Prentice-Hall, Inc., Englewood Cliffs, New Jersey, 1965).

Whitten, R.C. and I.G. Poppoff (1971), Fundamentals of Aeronomy, (John Wiley and Sons, Inc., New York, 1971), 247-252.